A STUDY OF THE EFFECT OF
CURVATURE
ON
FULLY DEVELOPED TURBULENT FLOW

Thesis by

Frank Wattendorf

In Partial Fulfillment of the Requirements for the Degree of

Doctor of Philosophy

California Institute of Technology

Pasadena, California

1933

A Study of the Effect of Curvature on

Fully Developed Turbulent Flow

ABSTRACT

In aeronautics we are especially interested in the
flow of air adjacent to surfaces, such as airfoils. There
are two main types of flow of real fluids, laminar and tur-
bulent, and it is turbulent flow which is of practical import-
ance in aeronautics. We should like to be able to predict the
skin friction and flow conditions for any surface of any shape.
There has recently been much success with the problem of pre-
dicting flow along a flat plate parallel to the direction of
flow, and the problem was attacked by investigation of fully
developed turbulent flow in straight channels, and direct
application of the semi-empirical laws obtained, to the flow
along a flat plate. However, surfaces met with in practice
are, in general, curved, so that it would be important to be
able to predict the effect of curvature on turbulent flow.
Most of the previous work in curved flow, however, has been
with curved pipes and channels where the behavior of the flow
was complicated by secondary vortices.

The present work had the purposes of isolating as
far as possible the effect of curvature on a fully developed
turbulent flow, with two dimensional mean motion. The curved
channels used were 5 cm. in breadth and 90 cm. in depth, and
had straight entrance sections over 60 x breadth in length to
produce a fully developed straight flow before subjecting it
to the effect of curvature. Channel I had inner radius 45 cm.

and outer radius 50 cm., while channel II had inner radius 20 cm. and outer 25 cm. In addition, measurements were made in an appratus consisting of two concentric cylinders, the inner one of radius 20 cm. and rotating, the outer of radius 25.4 cm. and fixed. The curvature was made of the same order as channel II for purpose of comparison.

Measurements on the channels consisted of pressure drop along the channel walls at several speeds, velocity distribution at $30°$ intervals around the curved portion, velocity distributions at several speeds, and for channel II, determination of the shearing stress at the walls of one of the curved sections.

Measurements on the cylinders consisted of velocity distributions at two speeds and determination of shearing stress at the outer wall.

Evaluation of results included: calculation of resistance law, calculation of the shearing stress, distribution in radial direction across the curved portion, determination of the exponential law for the velocity distribution near the walls in the various cases, calculation of the "mixing length" 1, from turbulent exchange theory, and several dimensionless methods of plotting velocity distributions to show similarity between measurements in the channels and in the concentric cylinders.

Also included are calculations of the laminar flow distribution in a curved channel, and a discussion of Rayleigh's stability criterion.

It appears that the distribution of centrifugal force

has a strong influence on the stability of the flow, and affects materially the velocity distribution. The fact that similarity can be obtained for several cases by proper dimensionless reduction based on the effective breadth of the mixing region looks hopeful, and it remains for future investigations to determine more facts about the effective breadth of the mixing region.

SUBJECT OUTLINE

A. INTRODUCTION.

B. PREVIOUS WORK.

1. Hydraulic experiments. Distinction between two- and three-dimensional mean flow. Flow in channels of circular and square cross-section.

2. Wilcken: boundary layer in curved channel.

3. Maccoll and Wattendorf:

    a. Meeting of boundary layers.

    b. Fully-developed flow.

4. Wendt: rotating cylinders.

C. PRESENT WORK.

1. Description of apparatus.

    a. Channel and motor.

    b. Pitot tubes and manometers.

    c. Rotating cylinders.

2. Description of measurements.

    a. Measurement of total head and calculation of the static pressure from wall readings and measured total head distribution.

    b. Velocity distributions along the channel at one speed.

    c. Scale effect. Dimensionless velocity distributions at different velocities.

    d. Pressure drop measurements and resistance law.

C,

    2.

       f.   Measurement of wall friction by means of Stanton
tube.

       g.   Measurements with concentric cylinders.

3. Calculations and analysis of results.

       a.   Calculation of the velocity distribution in
laminar flow for present channel and also for one of
stronger curvature.

       b.   Rayleigh's stability criterion.

       c.   Calculation of τ -distribution for curved channel.

       d.   Calculation of the mixing length "l".

       e.   Power laws for the velocity distribution near
walls for the different curvatures and for the rotating
cylinders.

       f.   Universal laws for the velocity distribution
near the walls for the different cases.

D. CONCLUSION.

A.   INTRODUCTION.

The flow of ideal fluids has been the subject of thorough mathematical investigation for many years, but it is only in the last few decades that a systematic attempt has been made to study the flow of real fluids. There are two main types of flow of real fluids: laminar and turbulent, of which the latter is the more important in practice. In aeronautics we are especially interested in predicting skin friction of surfaces, breakaway of flow and related phenomena, which depend largely on the behavior of turbulent flow in the neighborhood of a surface. There has been much success with semi-empirical treatment of turbulent flow in straight channels and along flat plates. However, flow encountered in practice is subjected in general to the influence of pressure gradient and curvature. The effect of pressure gradient has already been investigated to some extent in convergent and divergent channels. The present work gives experimental data on the turbulent flow in two different curved channels, the object of which was to isolate as far as possible the effect of centrifugal force on turbulent flow and thereby give a deeper insight into the mechanism of the flow of real fluids.

B.   PREVIOUS WORK ON CURVED FLOW.

1. Hydraulic experiments.

Most of the previous experimental work on curved flow has been done as special engineering investigations of such problems as resistance loss in pipe bends, and flow in turbines and water channels. Most of the investigations have

been made in channels whose depth and breadth were of the same
order of magnitude--in other words the flow occurring was
mean
essentially three dimensional in character. The nature of
such flow, with its secondary longitudinal vortices has been
discussed to some extent by Lell[1], Isaachsen[2], Hinderks[3], and
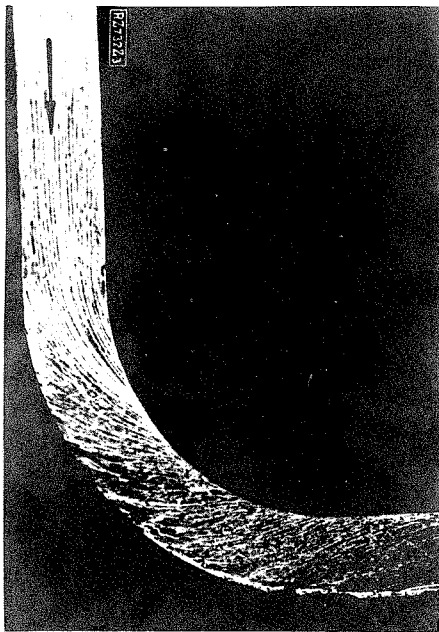Nippert[4]. Fig. 1 shows one of Hinderks' photographs of the
flow in a curved pipe, and Fig. 2
shows a schematic diagram of the
probable behavior of the three
dimensional curved flow. In the
center section, AA', the pressure
at the outer wall, p_2, is greater
than p_1, due to the centrifugal
force. At the top and bottom
surfaces, boundary layers will
form adjacent to the surfaces,
and the velocity will be decreased
so that the centrifugal force of
the fluid will be less than it is

Fig. 1

in the center section. Thus the fluid near the top and bottom
surfaces will be forced inwards, since the pressure gradient
along the radius will be unchanged in the boundary layer, and
will be the same as in the center. This gives rise to a cir-
culatory motion of two longitudinal vortices, whereby the
fast-moving particles in the center section tend to travel
outward, are diverted along the walls toward the upper corners,
and from there toward the inner wall, where they tend to collect

and form a so-called dead water region.

If, however, the depth of the channel is large compared with the breadth, the influence of the top and bottom boundaries on the flow is negligibly small and the behavior of the flow is quite different. The distribution of the centrifugal force has an unstabilizing effect on the fluid layers near the outer wall as will be discussed later. Thus the mixing process will be increased near the outer wall and will be decreased near the inner wall. The stability behavior may be considered analogous to that of motion in the atmosphere under different temperature gradients, where the temperature gradient plays an analogous role to that of the centrifugal force. When warmer layers are moving over colder layers, the system is stable, and the mixing is small, while if the colder layers move above the warmer, the system is unstable and mixing is increased.

2.   Betz-Wilcken experiments.

A series of experiments on so-called two-dimensional flow in curved channels was started by Betz in 1927. Wilcken[5] made the first investigations on the boundary layer flow in a series of curved channels. In each case the channel depth was large in comparison to the breadth in order to avoid the formation of the above mentioned secondary vortices. Wilcken found that the boundary layer on the concave outer surface developed much more rapidly than on the convex inner surface, which seems to confirm the supposition that the mixing is stronger at the outer wall. However, Wilcken dealt with two boundary layers separated by potential flow, and since the flow never reached a fully developed state, evaluation of

results was difficult. In the fully developed state the mean velocities are parallel to the walls and depend only upon the coordinate normal to the walls.

3. Maccoll-Wattendorf experiments.

In 1929 J. W. Maccoll and the present writer used a modified form of the Wilcken apparatus to study the further development of the flow after the boundary layers have come together. The channel was 3 cm. wide and 50 cm. in outer radius, and the boundary layers came together at about the 90° position. Fig. 3 shows the development of the velocity distribution. It is seen that the velocity profile undergoes a change after the meeting of the layers, but that the flow has not yet reached a fully developed state. In order to obtain a fully developed flow, a straight channel two meters in length was built before the curved channel so that the flow was already developed before it entered the curved portion of the channel. The velocity profiles are shown in Fig. 4, and indicate the approaching of a final state. The measurements were of an introductory nature and indicated clearly the need for further systematic work. It was for this reason that measurements were made in an improved type of curved channel at the California Institute of Technology.

4. Rotating cylinders.

A rather interesting case of curved flow is that of flow between rotating cylinders. In this case there is no pressure drop and for small ratios of gap to radius the

conditions approach those of the so-called Couette case for straight flow. The laminar flow has been subject to many investigations, but turbulent flow has been studied very little up to the present time. G. I. Taylor especially has studied the flow between rotating cylinders, both theoretically and experimentally.

Recently H. Wendt in Gottingen has investigated the turbulent flow of water between rotating cylinders. There is a great difference in the nature of the distribution depending on the relative direction and magnitude of rotation of the cylinders. Fig. 5 illustrates the nature of the flow when one of the cylinders is held stationary.

Except for the absence of pressure drop in the direction of flow, the flow near the stationary outer cylinder with the inner cylinder rotating should be analogous to the flow at the outer concave wall of the curved channel, while if the inner cylinder is fixed and the outer rotating the flow near the inner cylinder should be analogous to the flow near the curved inner wall of the curved channel.

The first case, that of inner cylinder rotating and outer cylinder stationary was investigated to some extent in an apparatus described in a later section. Mr. J. M. Nordquist cooperated with the author on the measurements with this apparatus, and is now extending the experiments to an investigation of surface roughness.

C. PRESENT WORK.

1. Description of apparatus.

a. Channels and motor.

Investigations were made in two different channels, designated I and II. Channel I is shown schematically in Fig. 6. The channel has a breadth of 5 cm. and a depth of 90 cm., so that the ratio of depth to breadth is 18:1. The ratio was chosen large to avoid as much as possible any disturbing influence of the top or bottom on the flow, in other words to avoid the formation of longitudinal vortices mentioned in section B-1. The channel consisted of the following main parts.

1. A bell shaped intake for the purpose of providing a smooth entrance. A honeycomb was built into the large portion of the funnel to straighten out eddies entering from outside.

2. A straight section 305 cm. long, for the purpose of building up the flow into a fully developed state. This length is 61 times the channel breadth and previous investigations have found 50 b to be sufficient for producing a fully developed flow.

3. The curved section, with the walls bent in concentric circular arcs, with the radius of the inner wall = 45 cm. and the radius of the outer wall = 50 cm. The curvature extended through about 300° of arc, in order to obtain as far as possible a fully developed curved flow. This was an improvement over the author's Gottingen channel which extended only through 180°.

4. An exit cone fastened on to the curved channel through a 180° gooseneck, and formed the transition between the rectangular channel section of 90 cm. x 5 cm. to the propeller section 55 cm. in diameter. The semi-angle of divergence of the transition section was about 8°.

5. The propeller and motor unit was designed by Dr. A. L. Klein for use in a future small high speed wind tunnel. The motor was a ~~Sterling~~ G.E., three phase, variable frequency motor, delivering *15* H.P. at 9000 R.P.M. The motor speed was controlled by varying the frequency, and this method proved to be highly satisfactory. The propeller was a four bladed, adjustable pitch, steel propeller, 55 cm. in diameter.

The power unit was capable of producing air speeds up to 120 m.p.h. in this tunnel, but during experiments much lower speeds were used to avoid collapsing of the channel walls. Stiffeners were used on the straight section to minimize the sucking in of the walls.

Channel II, Fig. 7, was similar to Channel I except that the radii of curvature were 20 cm. for the inner wall and 25 for the outer. Also the straight entrance channel was modified in that the walls were made of two sheets of 5/16" plymetal, making a much more rigid structure, and avoiding the necessity of using stiffeners. The entrance length was shortened slightly from 305 cm. to 285 cm., which is still 57 times the breadth, and sufficient for producing a fully developed flow.

Note: Mr. G. S. Lufkin was largely responsible for the construction of channel I, as well as preliminary measurements. CIT Master's Thesis 1931.

b. Pitot tubes and manometers.

Fig. 8 shows some of the pitot tubes used in the investigation. Tube a is one of the tubes for measuring total head. It consists of a 3/32" copper tube, bent at right angles, with a short length of hypodermic needle, .76 mm. in diameter carefully soldered into its tip. The total length of the tip was 38 mm. Two such tubes were used, one bent slightly so that the tip would come into good flat contact with the inner wall, and a similar one adapted to use at the outer wall.

Some experiments were made with the small Prandtl tube c, and also with a static tube not shown, but the results were not used, since a method for calculating static pressure was found to be more satisfactory, as explained in section C-2-a.

The so-called Stanton type tube b was used for investigations of total head very close to the walls. It was made by carefully flattening the end of a 3/32" copper tube. A piece of .001" shim stock was inserted in the end during the flattening process in order to avoid closing of the air passage. The outside dimensions of the tube were about .3 mm. x 3 mm. and inside about .15 mm. x 2.5 mm. The exact dimensions are not important since the effective center was determined during the measurements.

The tubes were moved through the tunnel by means of a hand operated micrometer, shown in Fig. 9. The measuring stations on the channels are shown in Figures 6 and 7. At each station there were three screws projecting outwards from the channel to accomodate the micrometer. The pitot tube

could then be inserted through a suitable hole in the channel wall and fastened to the micrometer. There were observation holes in the wooden top of the channel above each measuring station, so that the position of the tube could be properly adjusted.

The measuring stations were situated halfway between the top and bottom of the channel. At each station there was a small orifice in the wall, even with the tip of the pitot tube and displaced 2.5 cm. vertically from it, for the purpose of giving the static pressure at the walls.

Two micromanometers were used for the pressure measurements. They were designed by Dr. A. L. Klein and are described in the report by Millikan and Klein[6]. They were found to be very satisfactory, even for very low heads.

c.   Rotating cylinders.

The sketch of the rotating cylinder apparatus is shown in Fig. 10. It consists chiefly of an aluminum pulley, with polished surface, 20 cm. in radius and with a 30 cm. face, driven by a small Sterling three phase, variable frequency motor, delivering 0.1 H.P. at 3000 R.P.M. It is built into a wooden cylindrical housing, lined with a smooth galvanized iron sheet, so that the inner surface of the housing is concentric with the pulley, with a 5.4 cm. gap between. During measurements a cover was clamped on to the apparatus so that the air in the space between the cylinders was shielded from outside disturbance as much as possible.

The measurements were made with the same micrometer, pitot tubes and manometers as for the curved channels.

2. Description of measurements.

a. Measurements of total head and calculation of static pressure.

Instead of using a pitot-static tube for velocity measurements, closer distances to the wall could be obtained by measuring the total head and static pressure separately. The tubes have already been described. After preliminary work with the static pressure tube, however, it was decided to calculate the static pressure distribution from the readings obtained at the static orifices in the walls. It had previously been found that static tubes tend to read too low in turbulent flow, and this fact may be seen if we consider the characteristics of a static tube. Fig. 11 shows the calibration curve of pressure reading versus direction of mean flow for the static pressure tube used. It is clear that if the tube is placed in an air stream of fluctuating direction, the mean value of the pressure reading will be lower than the maximum, the magnitude depending on the percentage of angular fluctuation of the flow. An additional error may also exist in the present case due to the curvature of the streamlines around the tube. At the wall orifices, however, the fluctuation normal to the wall must vanish, and the stream lines will be parallel to the wall, so that the readings given by the static orifices are probably reasonably accurate.

The method of calculating the static pressure distribution from the wall readings is as follows:

Let u and v, (Fig. 12) be the tangential and normal components of velocity in a curved flow at radius r from the
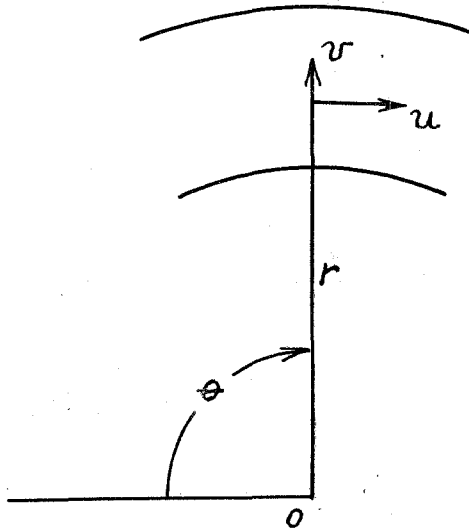
center of curvature, then

$$dp/dr = \rho u^2/r - \rho u \, dv/rd\theta$$

if we can neglect the effect of the apparent stresses of the type $\dfrac{\partial \tau}{r \partial \theta}$. The first term represents the centrifugal force, and the second term the pressure due to the normal component of velocity. The second term vanishes for fully developed flow, and even in the transition region is small against u^2/r.

Fig. 12

The calculation for the fully developed region where the second term may be neglected is as follows:

We have

$$dp/dr = \rho u^2/r \quad - - - - - - (1)$$

Now we assume that the measured value of the total head is accurate enough for our purpose

$$H = p + \tfrac{1}{2} \rho u^2 \quad - - - - - - - (2)$$

It follows from (2)

$$\rho u^2 = 2(H - p)$$

and substituting in (1) gives

$$dp/dr = (2/r)(H-p)$$

Using the pressure at one wall, say the inner wall, as reference,

$$d(p-p_i)/dr = (2/r)\left[(H-p_i) - (p-p_i)\right]$$

This is a linear differential equation of the first order whose

solution is

$$p - p_i = (1/r^2) \int_{r_i}^{r} (H-p_i)2r \, dr$$

H is taken from the measured total head distribution, p_i has been measured by a static orifice in the inner wall with good accuracy, and the function $(H-p_i)r$ is integrated graphically. As a check , the measured value of the outer wall pressure was in good accordance with our calculation.

b. Velocity distribution along channel at one speed.

The velocity is calculated from the curves of total head and static pressure according to the equation

$$H = p + \tfrac{1}{2}\rho u^2$$

The distribution for channel I is shown in Fig. 13 and for channel II in Fig. 14. It is seen that the velocity of the air is at first increased toward the inner wall, and that after this the velocity tends to increase again in the outer portion as though attempting to reach a distribution somewhat similar to potential "free vortex" flow with ur = const. throughout the center portion of the channel. More will be said later of the comparison of the fully developed distributions in the two different channels.

c. Scale effect.

Fig. 15 shows dimensionless velocity distributions for different mean velocities in channel I, and Fig. 16 in channel II. for 210° section. It is seen that for this small range of velocities the scale effect is quite small.

d. Pressure drop measurements and resistance law.

The pressure drop along the channels was deter-

mined by two different methods; first by connecting the static
wall orifices to a multiple manometer and recording the heights
of the alcohol columns on Osalite paper by exposing to a bright
light; and secondly by connecting each orifice in turn to a
single micromanometer through a multiple cock. The micromano-
meter proved to be more accurate. Pressure distribution curves
at several mean speeds for channel I are shown in Fig. 17, and
for channel II in Fig. 18. For channel I, the pressure drop
was measured only in the curved portion of the channel, while
for channel II, the straight section was measured as well. The
resistance coefficient λ for the channel was calculated according
to the definition,

$$\frac{\partial p}{r_c \partial \theta} = \frac{\lambda}{b} \cdot \frac{1}{2} \rho \, \bar{u}^2$$

where $\bar{u}$ = mean velocity, b = channel breadth and r_c = radius of
center line of the channel. Fig. 19 shows the result. It is
seen that the resistance coefficient for the straight entrance
is slightly lower than the Blasius law for straight pipes with
circular cross-section, and that the curved portion of the
channel has a resistance coefficient only slightly higher.
Higher resistance coefficients obtained in pipe bends of about
the same curvature may probably be attributed to the secondary
vortices of the three dimensional mean flow.

  e. Measurement of wall friction.

  As will later be shown, the wall friction τ_0 is not
uniquely determined by the pressure drop along the channel,
although the distribution may be calculated if the value of τ
at the one point is known. Therefore it is of particular im-
portance to determine experimentally the approximate value of

at the walls. The measurements were made with the Stanton
type tube, previously described.

For ~~the~~ orifices of such small dimensions, Stanton
found ^that^ the total head reading of the tube does not correspond
with the total head at the geometrical center of the tube, but *with*
the pressure at an "effective" center, at a distance δ^* from
the wall of the channel, when the tube is in contact with the
wall. Stanton determined the effective center by calibrating
the tubes in a channel where the flow was laminar in character.
For the present experiments, however, an approximate method
was used, as follows:

The shearing stress τ_0 at the wall of the straight
entrance section is determined by the pressure drop,

$$\tau_0 = b/2\,(dp/dx)$$

where b is the breadth of the channel. In the region quite
close to the wall we have a so-called "laminar sub-layer",
where the shearing stress is given essentially by the formula

$$\tau_0 = \mu(\partial u/\partial y)_0$$

μ is the coefficient of viscosity and $(\partial u/\partial y)_0$ represents
the velocity gradient at the wall.

If we define the distance from the wall ^to^ the effect-
ive center as δ^*, and the reading of the total head of the tube
as H^*, then the effective velocity is given as

$$\tfrac{1}{2}\rho\,U^{*2} = H^* - p$$

where p = the measured static pressure at the wall.

We have then for τ_0 approximately

$$\tau_0 = \mu\,(U^*/\delta^*)$$

from which δ^* may be calculated, since τ_0 is known for the
straight channel. Now we assume that δ^* is the same function

of U^*, and the breadth of the orifice of the Stanton tube in the curved channel as has just been found in the straight channel, when in both cases the Stanton tube was in contact with the wall. γ_0 is determined from the measured U^* and the corresponding value of δ^* taken from the curve.

In each case δ^* is determined for several speeds so that the value of γ_0 can be plotted against the reference wall pressure, while the other physical parameters involved, such as the diameter of the orifice, and μ remain unchanged. Fig. 20 shows the curve δ^* against the wall pressure, Fig. 21 of U^* against wall pressure, and Fig. 22 γ_0 against wall pressure. The applications of this determination will follow in a later section.

f.   Measurements with concentric cylinders.

For comparison with the flow in the curved channel, measurements were made in the rotating cylinder apparatus. The inner cylinder rotates, the outer cylinder is fixed. The curvature was roughly of the same order as curved channel II, the inner radius being the same, with the gap between the cylinders being 5.4 cm. as against 5 for the curved channel. The measurements were made with the same total head tubes, as well as with a Stanton tube.

As far as the flow at the stationary outer wall is concerned, the curvature effect should be about the same. There is no pressure drop in this, the so-called Couette case.

For comparison with the curved channel, consecutive measurements were made with the Stanton tube, first at the outer wall of the curved channel, and then at the wall of the stationary outer cylinder. In order to obtain the condition

of the same wall friction, the speed of the inner rotating cylinder was adjusted until the reading of the Stanton tube was the same as for the curved channel, and this condition was found to occur when the velocity head of the so-called "free vortex" in the center region between the cylinders was the same as for the curved channel.

Fig. 23 shows the measured total head and calculated static pressure distribution for the cylinders. It is seen that the total head is practically constant throughout a large region, corresponding to the condition of "free vortex" flow. Dimensionless velocity distribution for two speeds are shown in Fig. 24.

The distribution of τ for the rotating cylinder may easily be calculated from the value measured at the outer wall by means of the Stanton tube, by means of the equation of constant moment of force,

$$\tau r = \text{const.}$$

and the value τ_i for the inner wall is

$$\tau_i = \tau_o r_o / r_i$$

As a check on the accuracy of the Stanton tube measurement, the value of τ_i for the inner cylinder obtained by the calculation first mentioned was compared with corresponding measurements of H. Wendt of Gottingen who actually measured the torque on the inner rotating cylinder in a similar experiment with water. The values check within 3%

3. Calculations and analysis of results.

a. Calculation of the velocity distribution in laminar flow for the present channel, and one of stronger curvature.

It was thought of interest to compute the laminar flow in a channel of the same dimension as the present channel II, to see how the shape compared with laminar flow in a straight channel. The analysis is as follows:
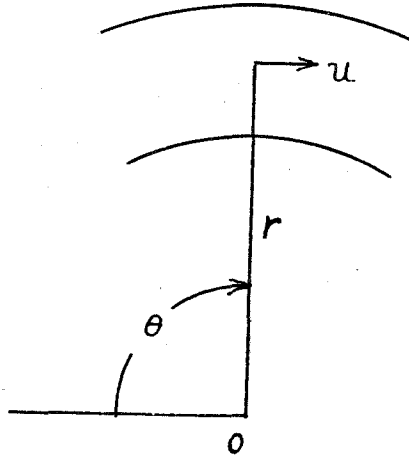
Referring to the diagram, Fig. 25, let u = the tangential velocity of flow, and v = the radial velocity = 0, for the fully developed case. Also $\partial u / \partial \theta$ = 0 when fully developed. Applying equations of momentum transport in tangential and radial directions, we have:

Fig. 25

In radial direction,

$$\frac{\partial p}{\partial r} = \frac{\rho u^2}{r} \qquad \text{----------- (1)}$$

In tangential direction,

$$-\frac{\partial p}{r \partial \theta} + \mu \left[\frac{\partial^2 u}{\partial r^2} + \frac{\partial \left(\frac{u}{r} \right)}{\partial r} \right] = 0 \qquad \text{----------- (2)}$$

Differentiating (1) gives

$$\frac{\partial^2 p}{\partial r \partial \theta} = 0$$

or

$$\frac{\partial p}{\partial \theta} = const. = C \qquad \text{----------- (3)}$$

and (2) becomes

$$\frac{C}{r} = \mu \left[\frac{\partial^2 u}{\partial r^2} + \frac{\partial \left(\frac{u}{r} \right)}{\partial r} \right]$$

Integrating, we have

$$C \ln r + C_1 2\mu = \mu \left(\frac{\partial u}{\partial r} + \frac{u}{r} \right)$$

Now, since

$$\partial (ur) / \partial r = r \cdot (\partial u / \partial r + u / r)$$

we can write

$$\partial(ur)/\partial r = c\frac{r}{\mu}\ln r + 2rc_1$$

$$ur = \int\left[\frac{r}{\mu}(c\ln r) + 2rc_1\right]dr + c_2$$

$$ur = c_2 + \frac{c}{\mu}\left[\frac{r^2}{2}\ln r - \frac{r^2}{4}\right] + \frac{2c_1 r^2}{2}$$

We have, then, as a final form of the velocity distribution,

$$u = c_1 r - (c_2/r) - (p'/2\mu)r \ln r$$

where

$$c = p' = \partial p/\partial \theta = \text{pressure drop per radian.}$$

The boundary conditions are

$$r = r_1 \text{------} u = 0,$$

$$r = r_0 \text{------} u = 0.$$

Substituting in the equation, we have

$$c_1 r_0 + \frac{c_2}{r_0} + K r_0 \ln r_0 = 0$$

$$c_1 r_i + \frac{c_2}{r_i} + K r_i \ln r_i = 0$$

where $k = p'/2\mu$

Solving for c_2

$$c_1 r_i r_0 + c_2 \frac{r_i}{r_0} + K r_i r_0 \ln r_0 = 0$$

$$c_1 r_i r_0 + c_2 \frac{r_0}{r_i} + K r_i r_0 \ln r_i = 0$$

Whence

$$c_2\left(\frac{r_i}{r_0} - \frac{r_0}{r_i}\right) + K r_0 r_i \ln \frac{r_0}{r_i} = 0$$

and

$$c_2 = -\frac{K r_0^2 r_i^2 \ln \frac{r_0}{r_i}}{r_i^2 - r_0^2}$$

Solving for c_1

$$c_1 r_0^2 + c_2 + K r_0^2 \ln r_0 = 0$$

$$c_1 r_i^2 + c_2 + K r_i^2 \ln r_i = 0$$

$$c_1 (r_0^2 - r_i^2) + K(r_0^2 \ln r_0 - r_i^2 \ln r_i) = 0$$

and

$$c_1 = -K \frac{r_0^2 \ln r_0 - r_i^2 \ln r_i}{r_0^2 - r_i^2}$$

We have then as the complete expression for u,

$$u = -K \frac{r_0^2 \ln r_0 - r_i^2 \ln r_i}{r_0^2 - r_i^2} \cdot r - \frac{K r_0^2 r_i^2 \ln \frac{r_0}{r_i}}{r_i^2 - r_0^2} \cdot \frac{1}{r} + K r \ln r$$

This can be simplified for calculation purposes as follows:

$$u = +K \frac{r_0^2 r_i^2 \ln \frac{r_0}{r_i}}{r_0^2 - r_i^2} \cdot \frac{1}{r} - K \frac{r_0^2}{r_0^2 - r_i^2} r \ln r_0 + K \frac{r_i^2}{r_0^2 - r_i^2} r \ln r_i + K r \ln r$$

But kr log r can be written as

$$K r \ln r \left[\frac{r_0^2}{r_0^2 - r_i^2} - \frac{r_i^2}{r_0^2 - r_i^2} \right]$$

since

$$\left[\frac{r_0^2}{r_0^2 - r_i^2} - \frac{r_i^2}{r_0^2 - r_i^2} \right] = 1$$

Combining terms we have

$$u = K \frac{r_0^2 r_i^2}{r_0^2 - r_i^2} \ln \frac{r_0}{r_i} \cdot \frac{1}{r} + K \frac{r_0^2}{r_0^2 - r_i^2} r \ln\left(\frac{r}{r_0}\right) + K \frac{r_i^2}{r_0^2 - r_i^2} r \ln \frac{r}{r_i}$$

and

$$u = K \left[\frac{r_0^2 r_i^2}{r_0^2 - r_i^2} \ln \frac{r_0}{r_i} \cdot \frac{1}{r} - \frac{r_0^2}{r_0^2 - r_i^2} \cdot r \ln\left(\frac{r_0}{r}\right) - \frac{r_i^2}{r_0^2 - r_i^2} \cdot r \ln \frac{r}{r_i} \right]$$

or,

$$u = K \frac{r_0^2 r_i^2}{r_0^2 - r_i^2} \left[\ln \frac{r_0}{r_i} \cdot \frac{1}{r} - \frac{r}{r_i^2} \ln \frac{r_0}{r} - \frac{r}{r_0^2} \ln \frac{r}{r_i} \right]$$

A simpler form for calculation purposes is:

$$u = K \frac{r_0^2 r_i^2}{r_0^2 - r_i^2} \left[\ln \frac{r_0}{r_i} - \left(\frac{r}{r_i}\right)^2 \ln \frac{r_0}{r_i} - \left(\frac{r}{r_0}\right)^2 \ln \frac{r}{r_i} \right] \frac{1}{r}$$

This expression, except for the constant factor, was cal-
culated for the two cases

1)) $r_i = 20$, $r_0 = 25$;

2)) $r_i = 5$, $r_0 = 10$,

and the calculated distribution is shown in Fig. 26. This
shows only a slight deviation from the parabola of the
straight flow, but the shift in maximum velocity is toward
the inner wall and the slope near the center seems to be
toward the potential flow. The measured turbulent flow has
the same tendency but to a much greater degree.

    b. Rayleigh's stability criterion.

    Rayleigh[7] has studied the stability of fluid in
curved flow, as follows.
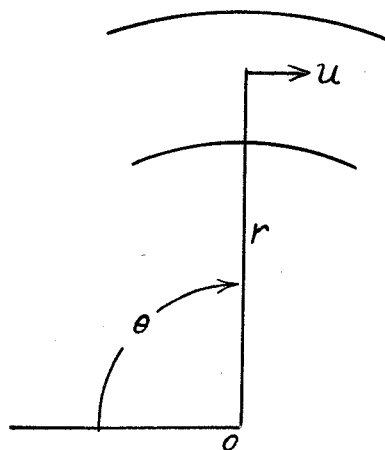
Consider the undisturbed flow
of a fluid in a curved path. If a
fluid element moving with tangential
velocity u at a distance r from
the center of curvature o, be dis-
placed by a disturbing force acting
along the radius, the moment of mo-
mentum taken around the axis perpen-
dicular to u through o, of the element
must remain unchanged, since there is

Fig. 27

no component of the disturbing force in the tangential direction. In the undisturbed flow, the pressure gradient along r is in equilibrium with the centrifugal force.

$$1. \quad \frac{\partial p}{\partial r} = \rho \frac{u^2}{r}$$

neglecting smaller order terms, such as friction.
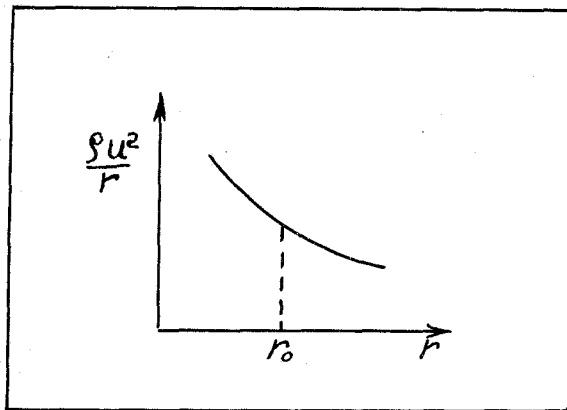
Let us consider now a flow where the product ur decreases with increasing r. The accompanying sketch shows the distribution of centrifugal force for such a case. If a fluid element at $r = r_0$ (be displaced) where it has the velocity u_0 outward along r, the requirement for constant moment of momentum is

Fig. 28

$$u_e r = u_0 r_0 \quad \text{or}$$

$$u_e = \frac{u_0 r_0}{r}$$

where u_e is the velocity of the fluid element at the time. The centrifugal force of the element is

$$2. \quad \rho \frac{u_e^2}{r} = \rho \frac{u_0^2 r_0^2}{r^3}$$

We have chosen, however, a flow with decreasing value of ur along the radius, so that $u < \frac{u_0 r_0}{r}$

for $r > r_0$ where u is the local fluid velocity.

Hence for the centrifugal force

$$3. \quad \rho \frac{u^2}{r} < \rho \frac{u_0^2 r_0^2}{r^3}$$

Substituting equation 1) and 2) in the above inequality we
have

$$4. \quad \frac{dp}{dr} < \frac{\rho u_e^2}{r}$$

Hence the centrifugal force of the displaced fluid
element is greater than the centripetal pressure gradient, and
the motion is unstable, because the tendency is for the dis-
placed particle to move further in the same direction. Con-
versely, if the displacement is inward, the centrifugal force
will be less than the centripetal pressure gradient, and the
element will be forced further inward.

In a similar manner we arrive at the conclusion that
in a flow where ur is increasing outward, the elements displaced
from their equilibrium positions will be forced back to their
positions, and the action will be stabilizing.

If we are dealing with a flow where ur = const. the
conclusion is that the stability is neutral.

Fig. 29 shows curves of ur for the curved channel II,
and the concentric cylinders. According to the above analysis
the flow at both inner and outer walls of the concentric cylin-
ders and at the outer wall of the curved channel is subject to
an unstabilizing effect, while at the inner wall of the curved
channel the effect is stabilizing. In the regions where we
find instability of the above outlined kind the mixing will be
increased, and therefore the region ur = const., which represents
a certain equilibrium condition, will be more rapidly approached.

This instability criterion has been first stated as
far as we know by Lord Rayleigh in 1916 and has been applied
and refined by taking the viscosity effect into consideration
by G. I. Taylor in his work on the instability of laminar flow

between two rotating cylinders in 1923. Later this instability has been found independently by Bjerknes and Solberg in the course of their meteorological investigations in 1927. L. Prandtl pointed out a similar theorem in 1929 at the Aachen Aerodynamics Congress.

c. Calculation of the τ distribution for the curved channel.

The distribution of the shearing stress τ for a fully developed curved flow may be calculated from a consideration of the moments of momentum about the center of curvature of the channel.

Consider the forces acting on a small element of fluid in a curved channel. Fig. 30 represents an element at radius r.. The flow is assumed fully developed, that is, there is no change of momentum in the tangential direction and the mean value of the normal component is everywhere $=0$. The only forces acting are pressure and shearing stress. If we take τ as the shearing stress, then the shearing force on the area formed by the arc $rd\theta$ and unit depth is
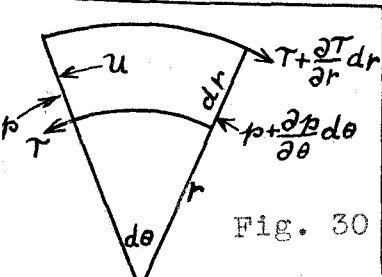
$$\tau rd\theta$$

and the moment of this force about the center is

$$\tau r^2 d\theta$$

If p = pressure, the moment of the pressure about the origin is $pdr \cdot r$.

Equating moments of force we have

Fig. 30

$$\tau r^2\, d\theta + \frac{\partial(\tau r^2)}{r}\, dr\, d\theta - \tau r^2\, d\theta =$$

$$pdr + \frac{\partial p}{\partial \theta}\, d\theta\, dr - pdr$$

or $\quad \dfrac{\partial (\tau r^2)}{\partial r} = \dfrac{\partial p}{\partial \theta} \cdot r dr$

Integrating

$$\int \dfrac{\partial (\tau r^2)}{\partial r} dr = \int \dfrac{\partial p}{\partial \theta} \ r dr$$

or $\quad \tau r^2 = \dfrac{\partial p}{\partial \theta} \ \dfrac{r^2}{2} + c$

where $\dfrac{\partial p}{\partial \theta}$ is taken as constant over the radius. This last assumption can be derived from the fact that u is independent of θ in the fully developed flow. We have only to differentiate the equation

$$\dfrac{\partial p}{\partial r} = \rho \ \dfrac{u^2}{r}$$

with respect to θ, which gives

$$\dfrac{\partial^2 p}{\partial r \partial \theta} = 0 \qquad \text{or} \quad \dfrac{\partial p}{\partial \theta} \text{ is}$$

independent of r.

The constant of integration may be determined if we know the value of τ at one point. If we take the point in the channel where $\tau = 0$ as reference, and call the radius at this point r_m, we have

$$c = - \dfrac{\partial p}{\partial \theta} \ \dfrac{r_m^2}{2}$$

and finally

$$\tau = \tfrac{1}{2} \dfrac{\partial p}{\partial \theta} \left[1 - \left(\dfrac{r_m}{r} \right)^2 \right]$$

The choice of r_m has been subject to some discussion, according to the definition of τ. For laminar flow in a curved path, we have

$$\tau = \mu \left(\dfrac{\partial u}{\partial r} - \dfrac{u}{r} \right)$$

where μ is the coefficient of viscosity of the fluid. It is customary to use an analogous expression for τ in a

turbulent flow, namely,

$$\tau = \rho \varepsilon \left(\frac{\partial u}{\partial r} - \frac{u}{r} \right)$$

where ε represents the "apparent" coefficient of kinematic viscosity, or "exchange coefficient" of the turbulent mixing process. From this point of view it would seem obvious that $\tau = 0$ when

$$\frac{\partial u}{\partial r} - \frac{u}{r} = 0$$

For straight flow, we have

$$\tau = \rho \varepsilon \frac{\partial u}{\partial y}$$

Prandtl introduced the so-called "mixing length" l or the mean distance which a fluid element travels before losing its identity. By means of "l", τ may be expressed

$$\tau = \rho l^2 \left(\frac{\partial u}{\partial y} \right)^2$$

By an analysis in which he assumes that a displaced fluid element in curved flow maintains its moment of momentum, Prandtl gives as the expression for τ in a curved flow[9]

$$1. \quad \tau = \rho \, l^2 \left(\frac{\partial u}{\partial r} + \frac{u}{r} \right)^2$$

whereby it is seen that $\tau = 0$ for $\dfrac{\partial u}{\partial r} + \dfrac{u}{r} = 0$

However, on the basis of the assumption that a displaced fluid element in curved flow maintains its vorticity, we obtain the expression

$$2. \quad \tau = \rho \, l^2 \left(\frac{\partial u}{\partial r} - \frac{u}{r} \right)^2$$

whereby $\qquad \tau = 0$ for $\dfrac{\partial u}{\partial r} - \dfrac{u}{r} = 0$

The importance of determining τ experimentally is evident, and it was for this reason that an approximate method

of determining τ_0 at the walls, by means of the Stanton tube
was developed for Channel II.

Curves for the distribution of τ in channel II for
the two cases corresponding to $\tau = 0$ at $\frac{\partial u}{\partial r} - \frac{u}{r} = 0$ and [$r_m = 21.2\,cm$]
[$r_m = 24.0$]
$\frac{\partial u}{\partial r} + \frac{u}{r} = 0,$ and also the distribution corresponding to the
measured wall values [($r_m \simeq 21.7$)] is shown in Fig. 31. It is seen that
the curve with the measured end points lies between the other
two, and is closer to the curve which has its zero point at

$$\frac{\partial u}{\partial r} - \frac{u}{r} = 0 \quad where \; r_m \simeq 21.2$$

Physically this may mean that since the different
expressions for τ are attempts at approximations to the true
conditions, they may both be partly right, and the actual
flow may be a combination of several processes, and be between
the two theoretical curves. The evaluation of results for
channel II were made on the basis of the curve corresponding
to the measured wall points. $(r_m \simeq 21.7)$

d. Power laws.

It has been found that for turbulent flow in straight
channels, the velocity throughout the greater part of the
channel may be expressed as an exponential function of the
distance from the wall.

$$u = y^{\frac{1}{n}}$$

n, for flow in channels at Reynolds numbers around 200,000
is about 7. However, it has been shown, chiefly by von Karman,
that the exponent is a function of the Reynolds number, and n
increases with Reynolds number, reaching 9 or 10 at
$R_n \sim 1,000,000$. The increasing exponent in this case corres-
ponds to the flattening off of the velocity distribution with

increasing scale. The flattening off of the velocity distri-
bution, would seem to indicate an increased mixing near the
walls, since with increased mixing the central velocity is sooner
approached than when the mixing is less. Fig. 33 shows the
velocity distribution near the walls of both curved channels,
as well as the straight section, for $Rn \hookrightarrow 100,000$ plotted logarithmically and
it is seen that fairly good straight lines can be drawn
through the points.

If we take $\frac{b}{r_0}$ as a measure of curvature where
b = channel breadth and r_0 = radius of curvature of the outer
wall, calling concave curvature positive and convex negative,
and plot the exponent n against the curvature for the dif-
ferent cases we get the result shown in figure 32. In accord-
ance with our stability criterion we see that increasing n
goes together with increasing instability, while decreasing n
goes together with increasing stability.

e. Universal laws.

Prandtl[1] introduced a dimensionless method of plot-
ting velocity distribution near the walls of a straight channel,
and Nikuradse[10] applied this to flow in straight pipes with
different wall roughnesses and found that all points for the
different conditions fitted well on a single curve which he
terms the universal velocity distribution near walls. The
result for the curved channel and concentric cylinders, plot-
ted in this dimensionless manner is shown in Fig. 34. Evident-
ly the universal law applies only to straight pipes and
channels because our points for the straight section fit
Nikuradse's curve whereas the other cases deviate system-

atically from it.

Another basis of similarity of velocity curves is a modification of the Stanton-Karman method of plotting. Karman obtains similarity in straight flow by plotting the function $\dfrac{U_{max} - u}{\sqrt{\tau_0/\rho}}$ against $\dfrac{y}{b}$ where b is channel breadth. We have modified this for the curved channel by using $u_{pot.} =$ the velocity which a potential flow would have at the considered point, whereby the potential velocity distribution is tangent to the actual curve at the point

$$\frac{du}{dr} = -\frac{u}{r}$$

The dimensionless velocity is taken as $\dfrac{u_{pot.} - u}{\sqrt{\tau_0/\rho}}$ where τ_0 is the measured wall value. The radial distance is made dimensionless by dividing by the so-called effective breadth "b_e". b_e is defined as the distance from the channel wall to the point where the potential velocity distribution is tangent to the measured velocity curve. b_{e_0} is the effective breadth for the outer wall region, and b_{e_i} for the inner wall.

The result is shown in Fig. 35. It is seen that there is good accordance between the outer walls of curved channel II and the outer stationary cylinder, and also accordance between the inner wall of the channel and the inner rotating cylinder. Straight flow however, falls outside, and it is interesting to consider that straight flow has no well defined effective breadth, in other words there is no distinct flattening out of the velocity curve at the channel center.

Conclusion

The measurements with these two channels of different curvatures, and with the concentric cylinders have shown the following general facts.

1. That there is only slight increase in channel resistance due to the curvature indicating that previous results with curved pipes were probably influenced greatly by the secondary vortices of three dimensional mean flow.

2. That the velocity distributions are strongly influenced by curvature and that the flow through the center region approaches the potential flow with the law $ur = $ const.

3. That Rayleigh's stability criterion predicts instability and increased mixing at the outer wall of the curved channels and both walls of the concentric cylinders, and stability at the inner wall of the curved channel. Consideration of the power laws and effective breadth bear out the criterion.

4. That similarity in the velocity profiles can be obtained with the flow in concentric cylinders of the same curvature by proper reduction, making use of the "effective breadth".

In conclusion it may be said that these experiments indicate the need of further systematic experiments on turbulent flow, with the attempt of isolating the various influences as much as possible and forming semi-empirical laws for them which may later be combined to apply to the problems of aero and hydrodynamics of practical importance.

REFERENCES

1.) Lell: Beitrag zur Kenntnis der Sekundärströmungen in gekrümmten Kanalen. Darmstadt Dissertation 1913.

2.) Isaachsen: Zeitschrift der V.D.I. 55 (1911)

3.) Hinderks: Zeitschrift der V.D.I. 71 (1927)

4.) Nippert: Forsch. Arb. a. d. Geb. d. Ing. wesen, 320 (1929)

5.) Wilcken: Turbulente Grenzschichten an gewölbten Flächen. Ingenieur Archiv, I:4, (1930)

6.) Millikan and Klein: Description and Calibration of the ten foot Wind Tunnel at the California Institute of Technology. A.S.M.E. Proceedings (1932)

7.) Rayleigh: On the dynamics of a revolving fluid. Vol. 6 Scientific Papers (1916)

8.) Prandtl: Verh. d. 2. Intern. Kongress f. Techn. Mech. Zürich - 1926

9.) Prandtl: Verh. d. Aachen Kongress - 1929.

10.) Nikuradse: Verh. d. 3. Intern. Kongress f. Techn. Mech. Stockholm (1930)

11.) Taylor, G.I.: Phil. Trans. A. Vol. 223, p. 289, 1922.

12.) Bjerknes and Solberg: Zellulare Trägheitswellen und Turbulenz. Videnskabsakademiets avhandlinger, I, No. 7, Oslo 1929.

Acknowledgement

The author wishes to express his sincere appreciation for the inspiration and guidance of Dr. von Karman during these investigations, to Dr. W. Tollmien for his kind interest and advice, to Dr. A. L. Klein for help and suggestions regarding apparatus, and to all others of the Guggenheim staff.
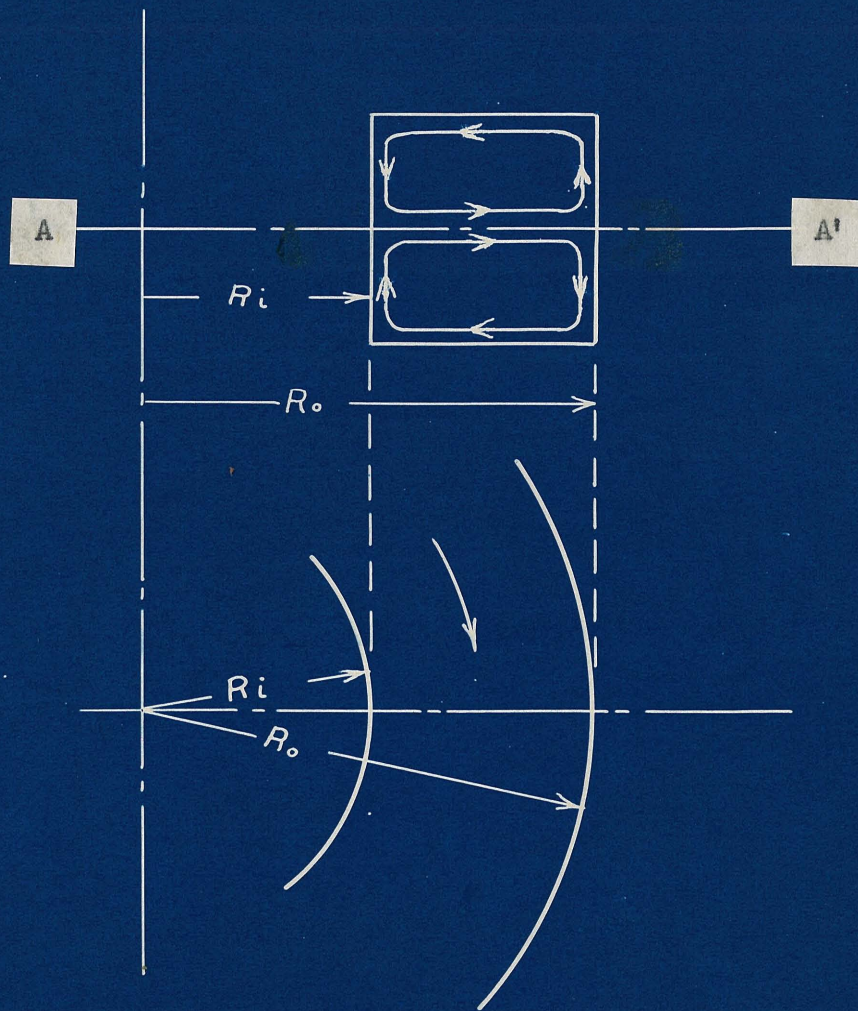
LONGITUDINAL VORTICES IN CURVED
CHANNEL OF SQUARE CROSS SECTION

180°

150°

120°

90°

60°

30°

0°

180°

150°

120°

90°

60°

30°

0°
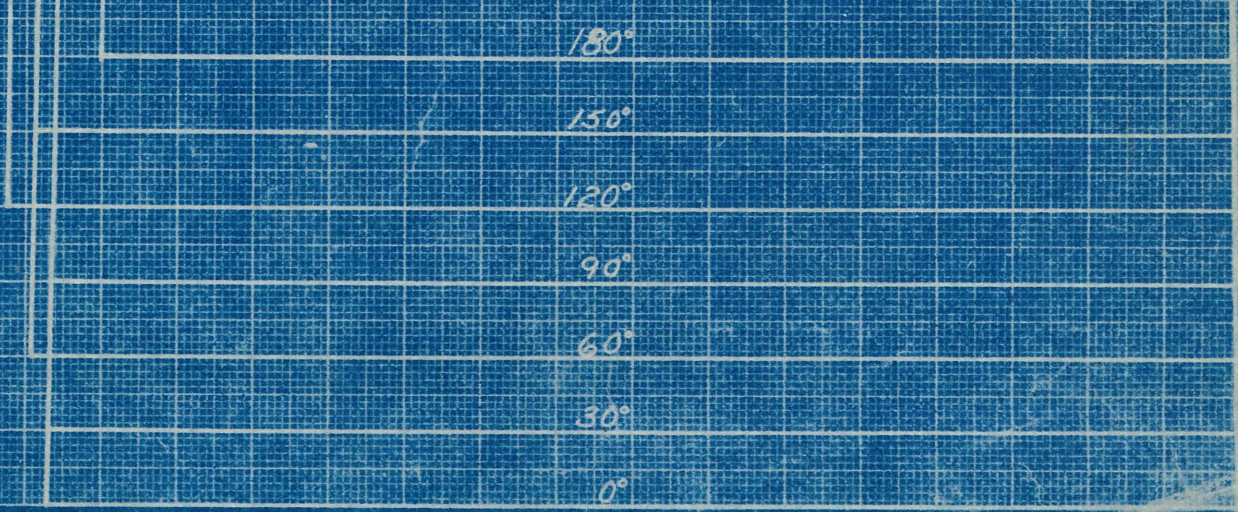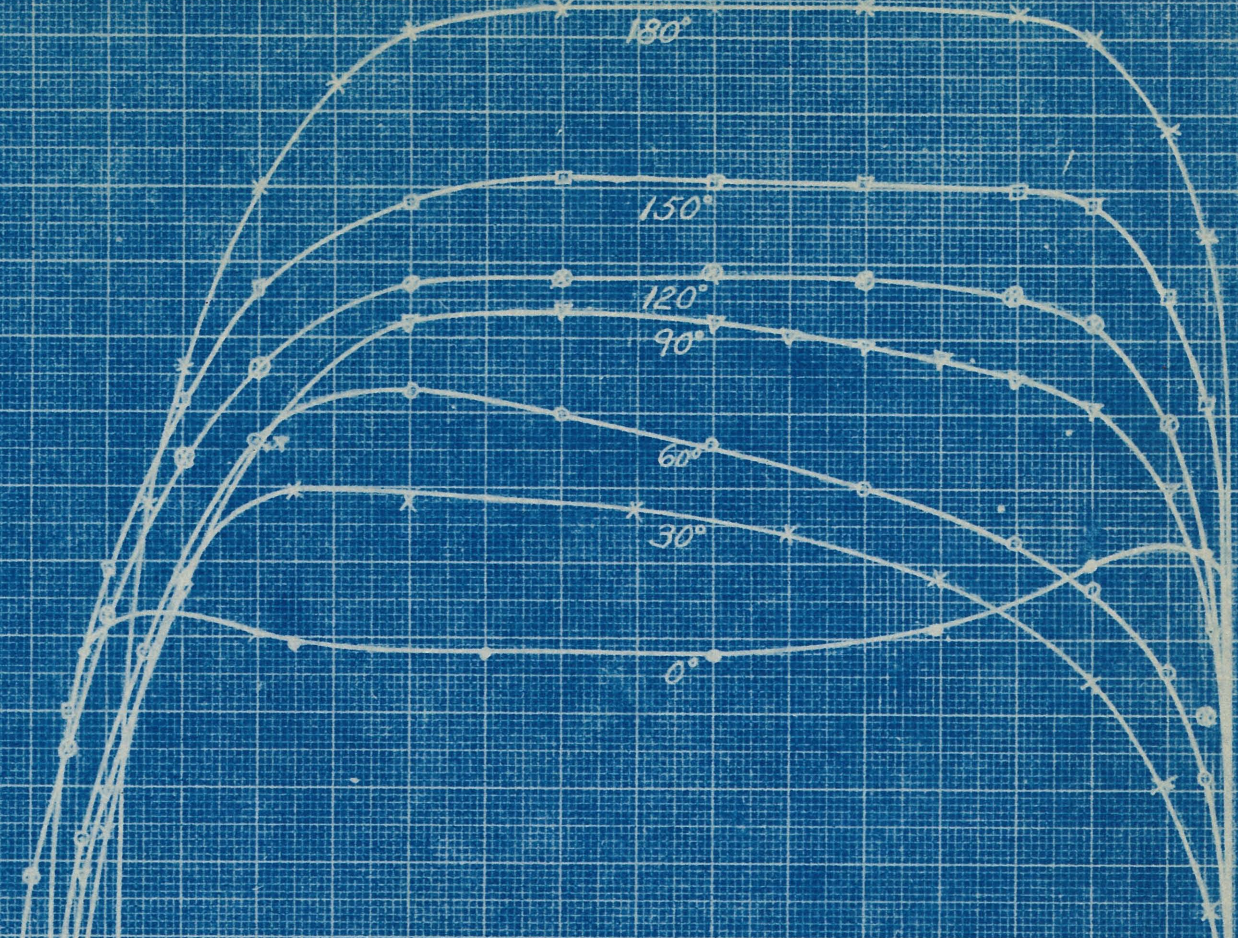
468   472   476   480   484   488   490   500
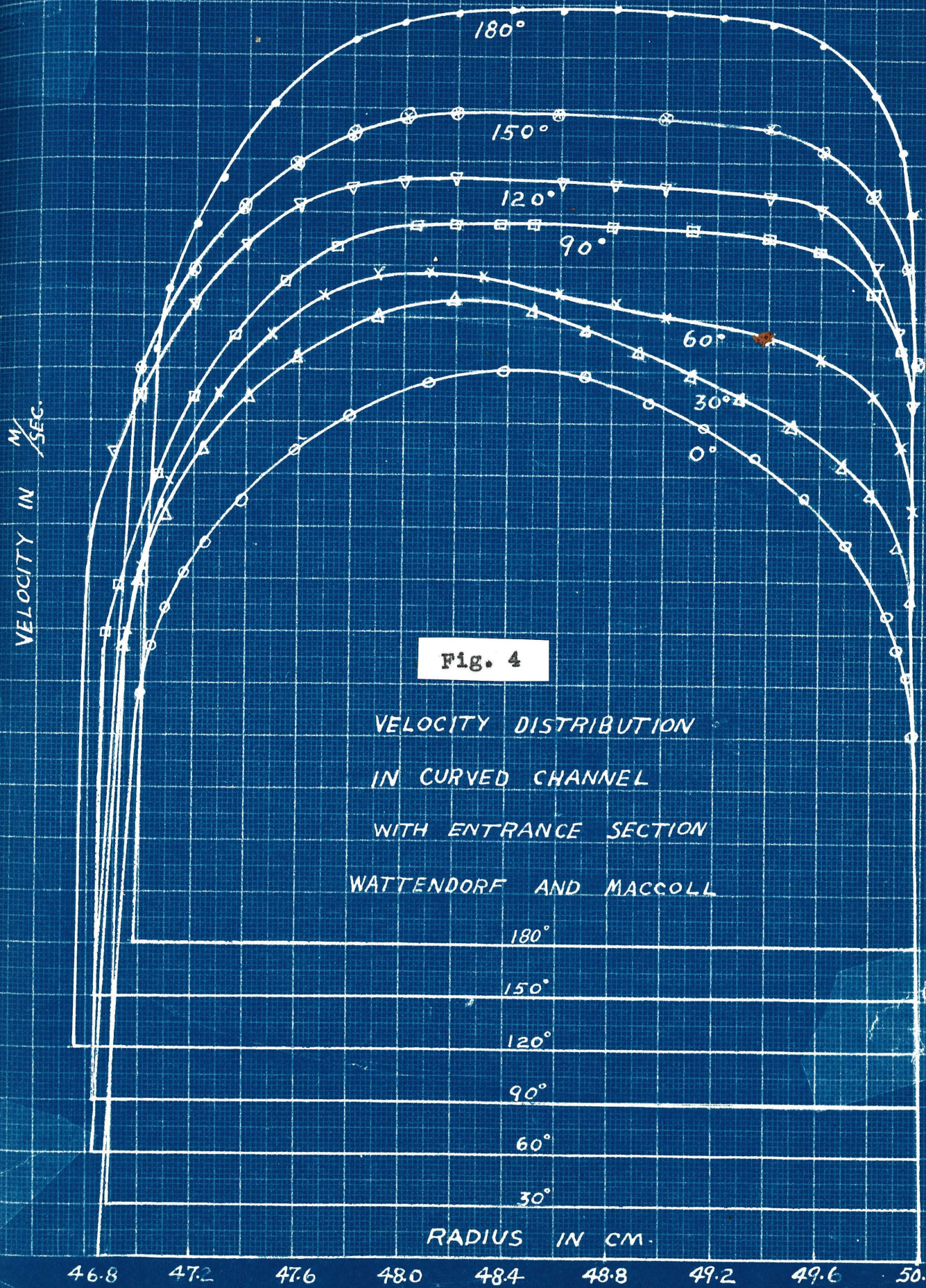
Fig. 4

VELOCITY DISTRIBUTION
IN CURVED CHANNEL
WITH ENTRANCE SECTION
WATTENDORF AND MACCOLL

RADIUS IN CM.

TANGENTIAL VELOCITY
DISTRIBUTION BETWEEN
CONCENTRIC CYLINDERS

CURVED CHANNEL I

Cross Section

90 cm.

5 cm.

45 cm.R

305 cm.

45 cm.

0°
30°
60°
90°
120°
150°
180°
210°
240°
270°
280°
210°

6 C
6
5
4
3
2
1

10
50
50
50
50
50
50
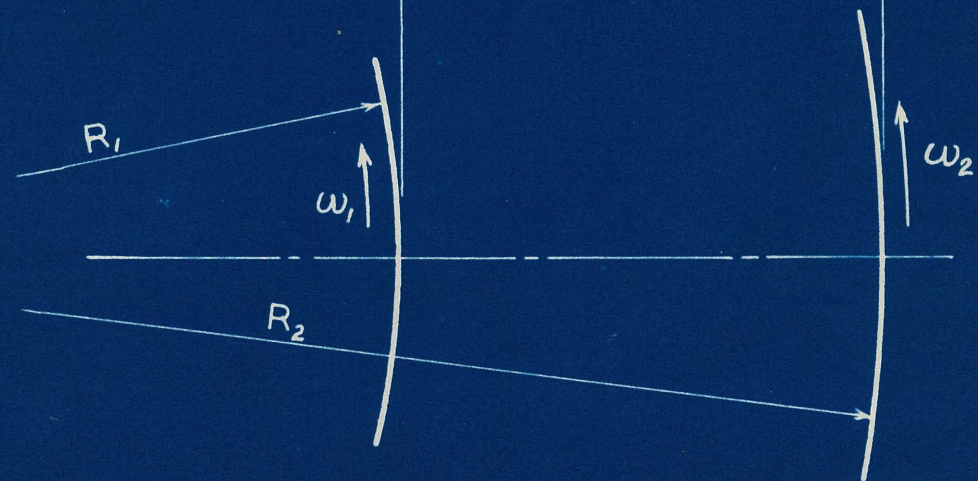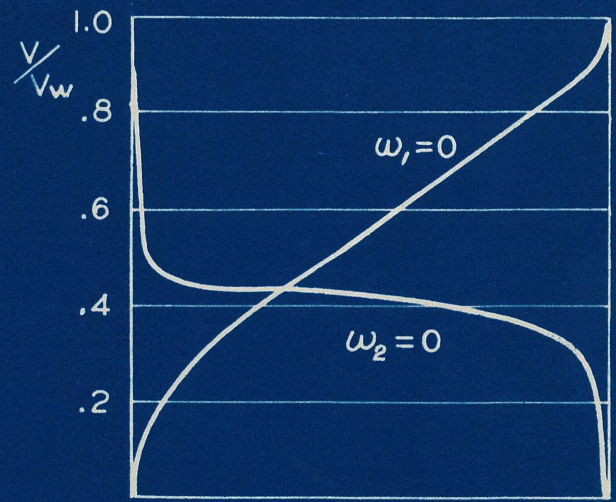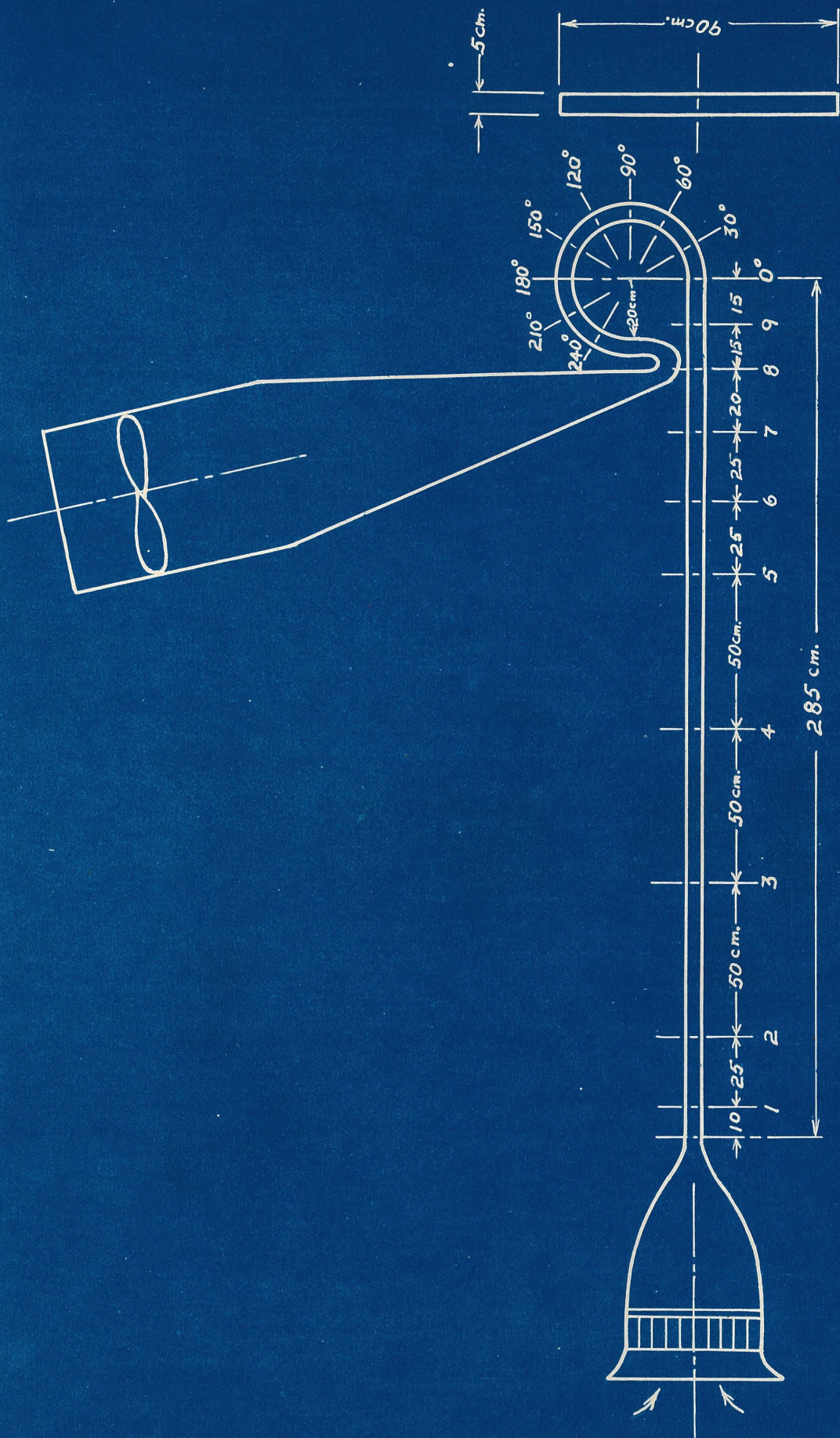
CURVED CHANNEL II

Fig. 8

Fig. 9

5 cm.

20 cm.R

30 cm.

Fig. 10

ANGLE OF DEFLECTION
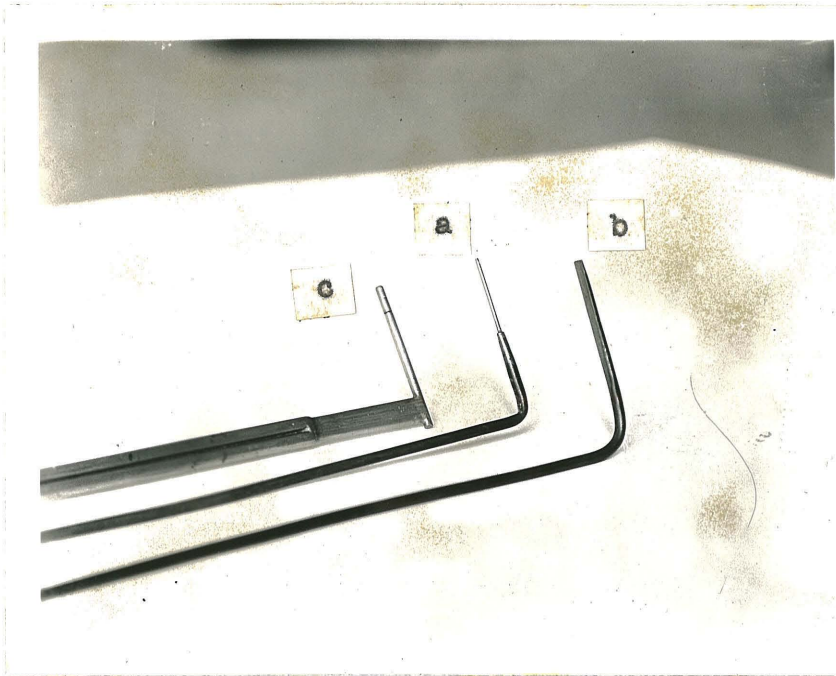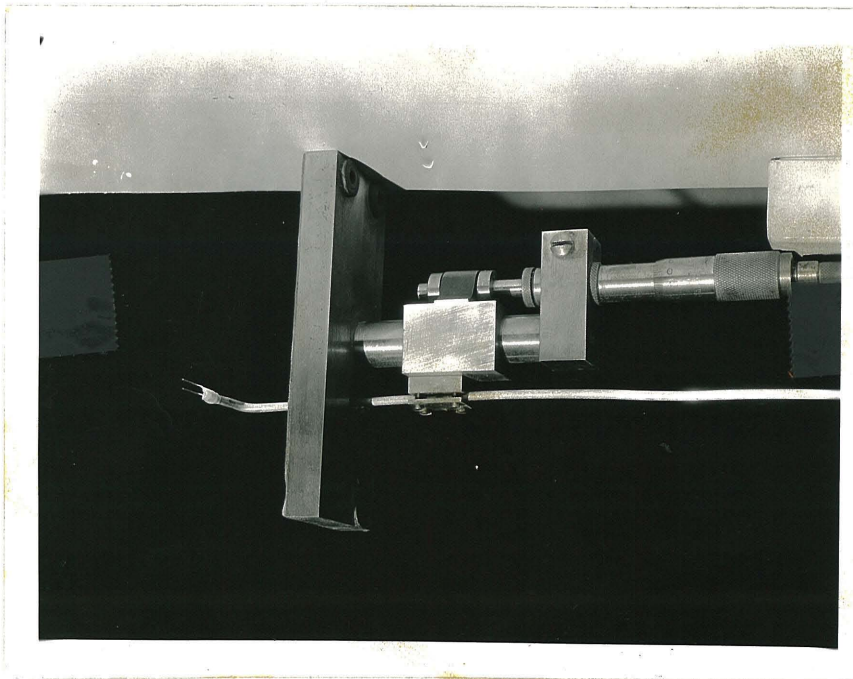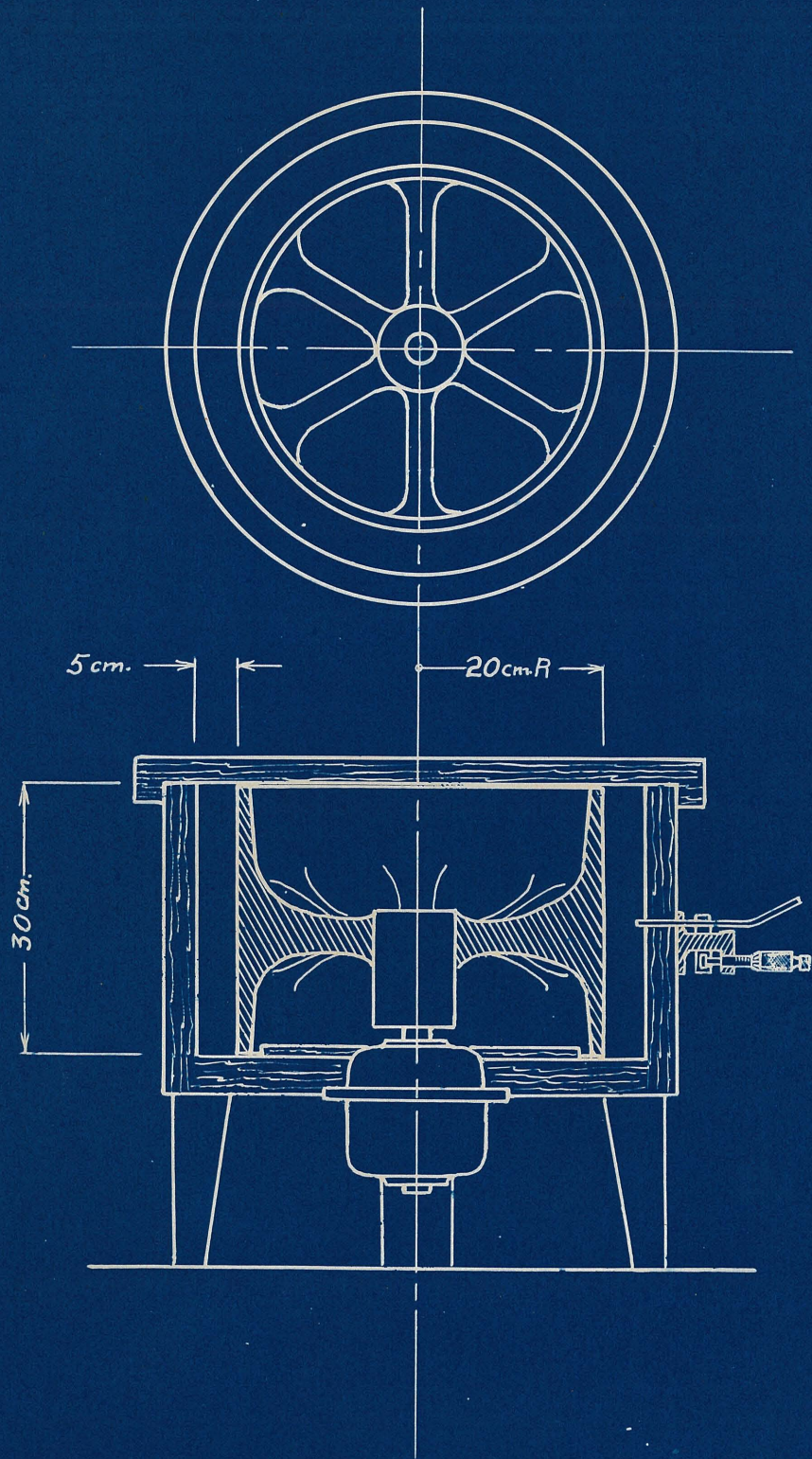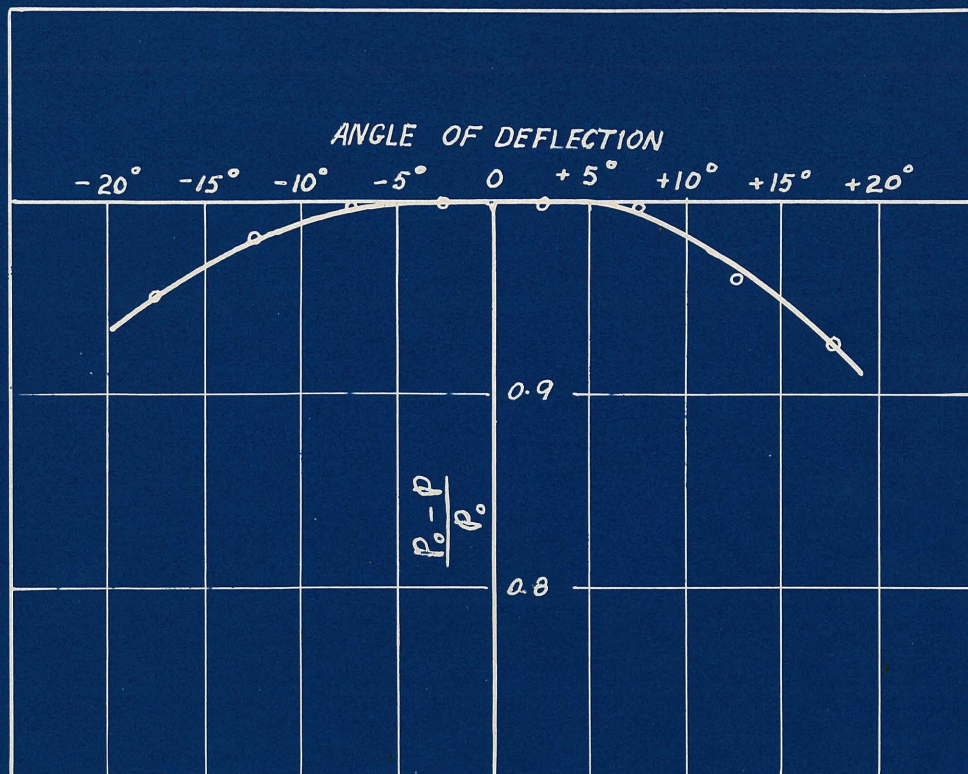
CALIBRATION OF STATIC TUBE FOR
DEVIATION OF ANGLE
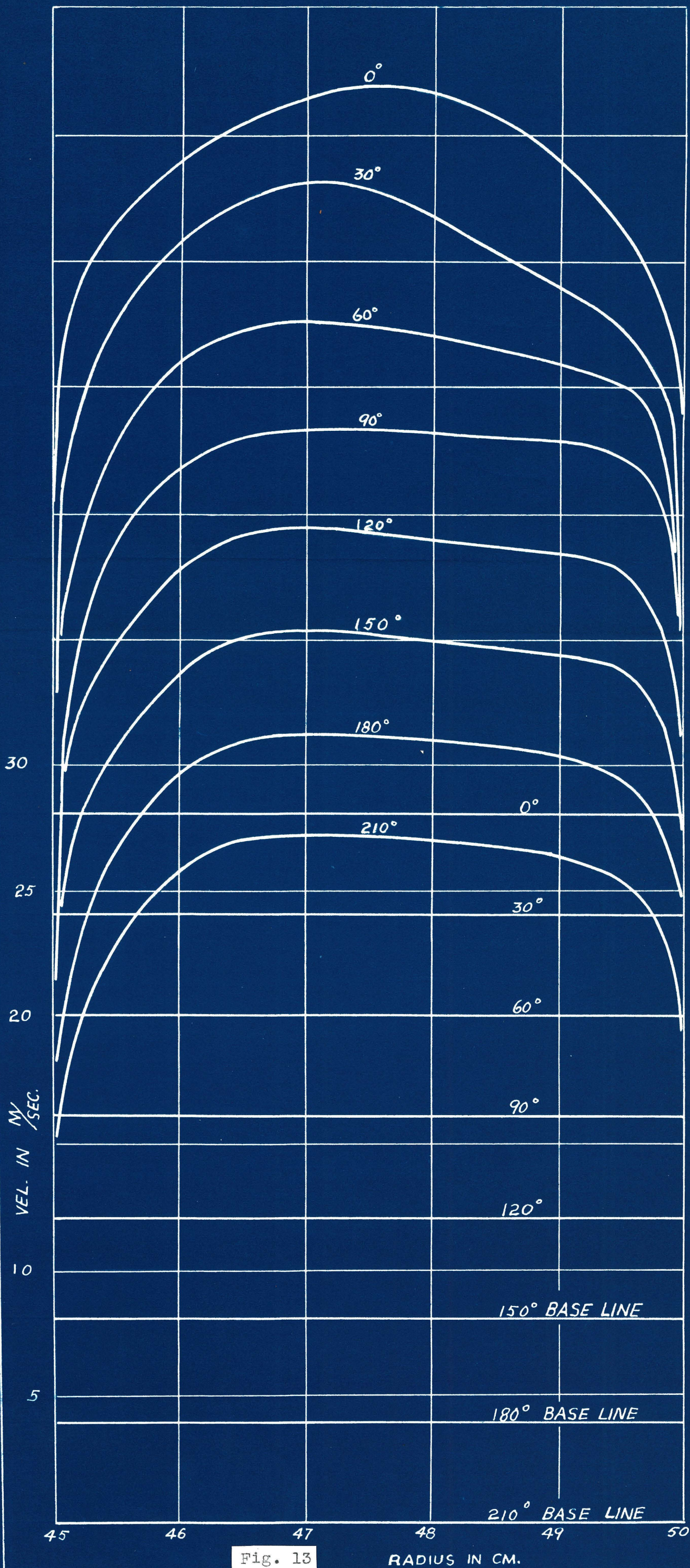
Fig. 11

Fig. 13

VELOCITY DISTRIBUTION IN CURVED CHANNEL I

Fig. 14

VELOCITY DISTRIBUTION IN CURVED CHANNEL II
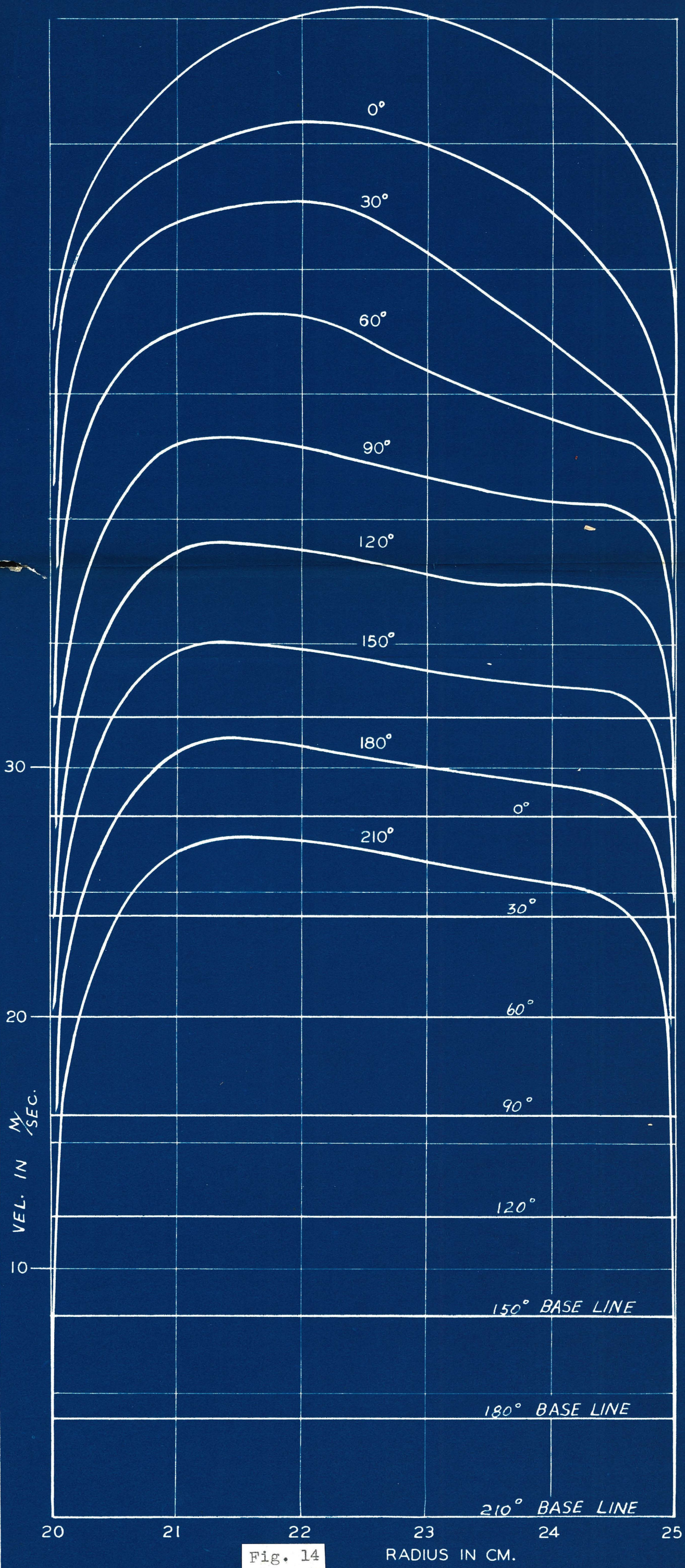
DIMENSIONLESS VELOCITY DISTRIBUTION IN CURVED CHANNEL I

RADIUS IN Cm.
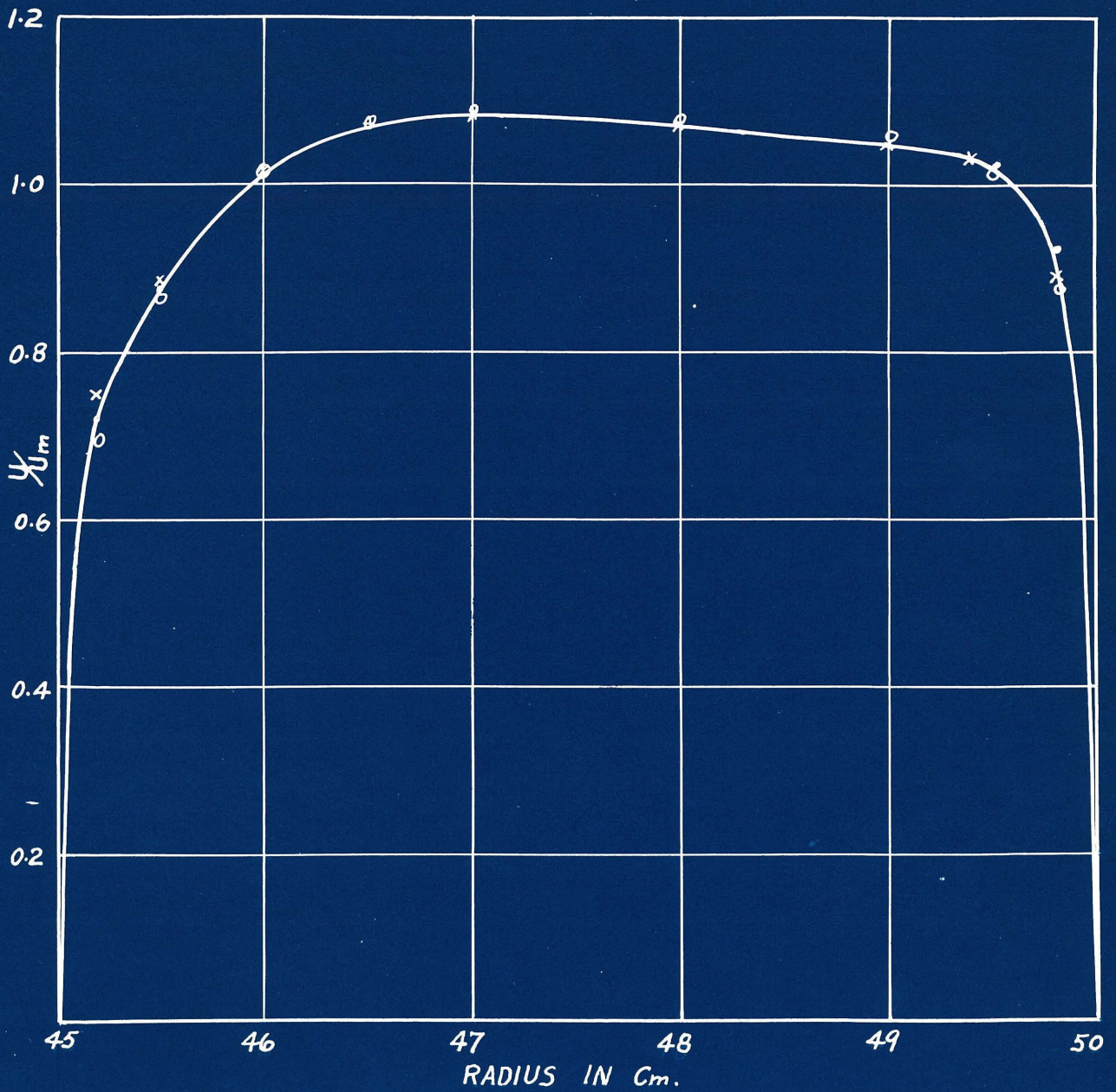
o $U_m = 8.44$ $\frac{M}{SEC.}$
x $U_m = 17.65$ $\frac{M}{SEC.}$
△ $U_m = 25.00$ $\frac{M}{SEC.}$

DIMENSIONLESS VELOCITY DISTRIBUTION IN CURVED CHANNEL II

Fig. 16

DEGREES FROM 0° SECTION

PRESSURE DROP ALONG WALLS
CHANNEL I
○   10 m/sec
△   15.5 m/sec
✳   25 m/sec

outer wall
inner wall

WALL PRESSURE IN mm WATER
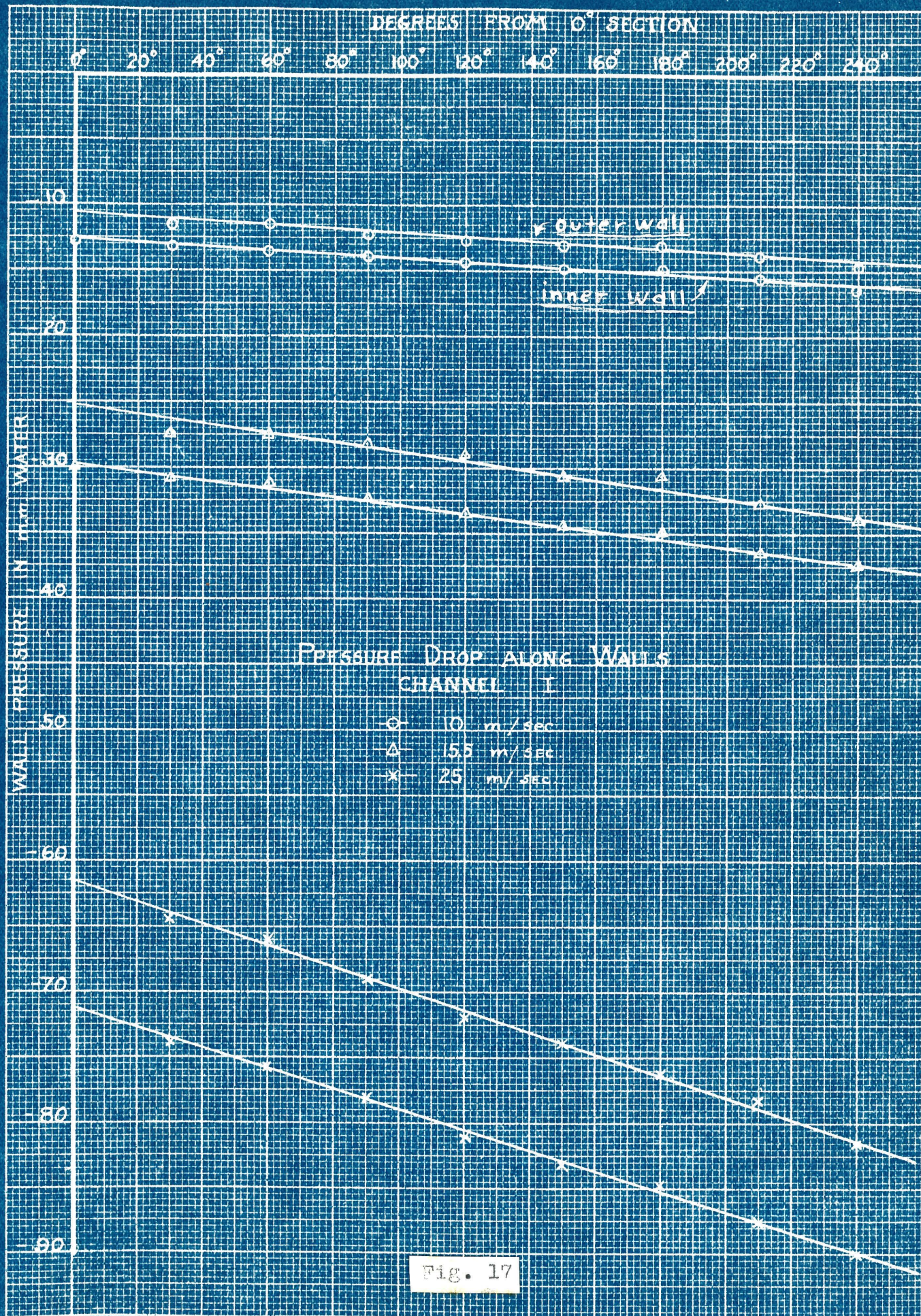
Fig. 17

PRESSURE IN mm. OF WATER

Cm. FROM ENTRANCE

STRAIGHT SECTION

CURVED SECTION

DEGREES FROM 0° SECTION

$\bar{U}=27.10 \frac{M}{SEC.}$

$\bar{U}=18.00 \frac{M}{SEC.}$

$\bar{U}=12.36 \frac{M}{SEC.}$

$\bar{U}=7.50 \frac{M}{SEC.}$

inner wall

outer wall
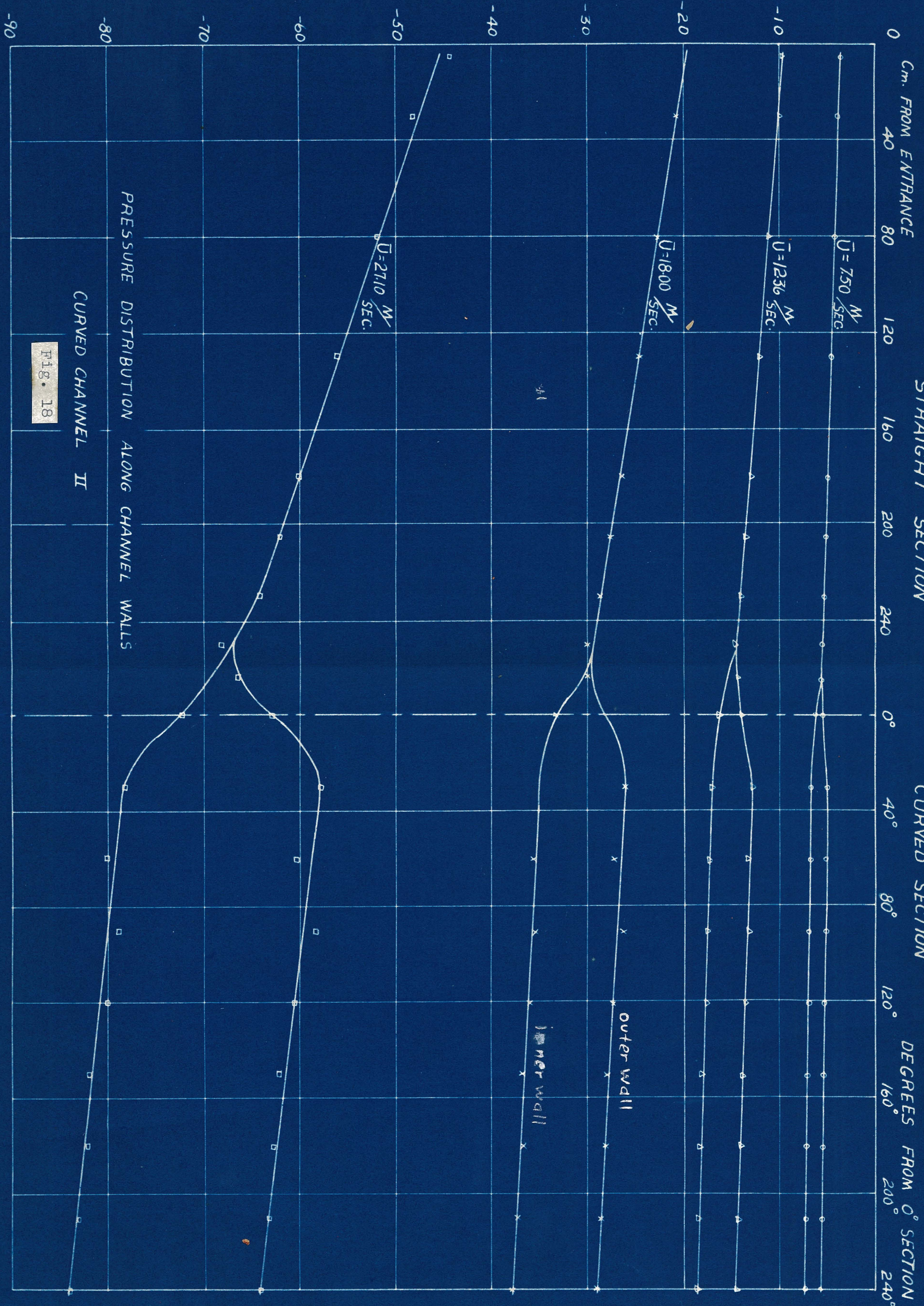
PRESSURE DISTRIBUTION ALONG CHANNEL WALLS

CURVED CHANNEL II

Fig. 18

RESISTANCE LAW FOR CURVED CHANNEL II

x ——— Straight Sections
⊙ ——— Curved Section

Blasius Law

Log (1000λ)

Log R

Fig. 19

Fig. 20
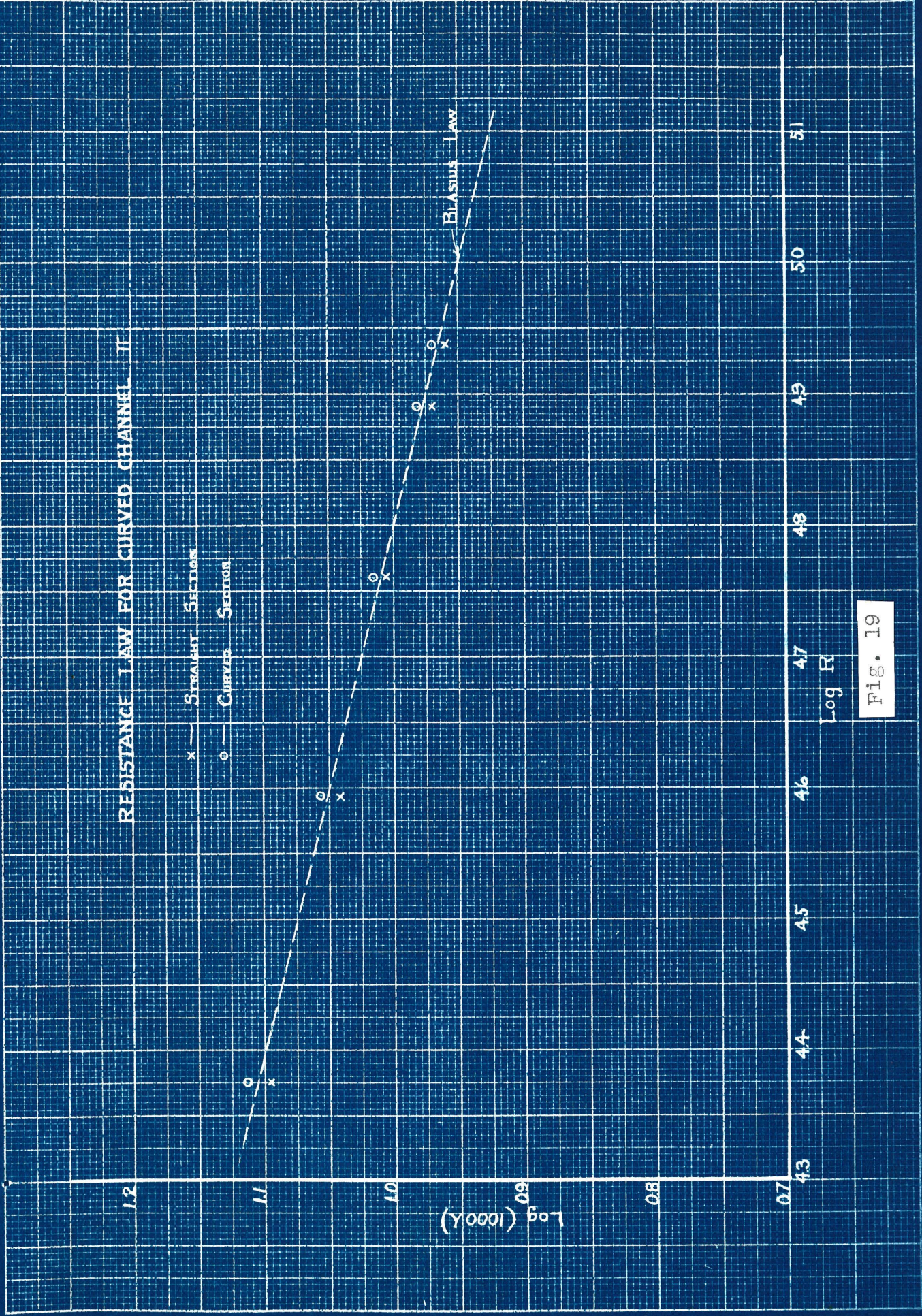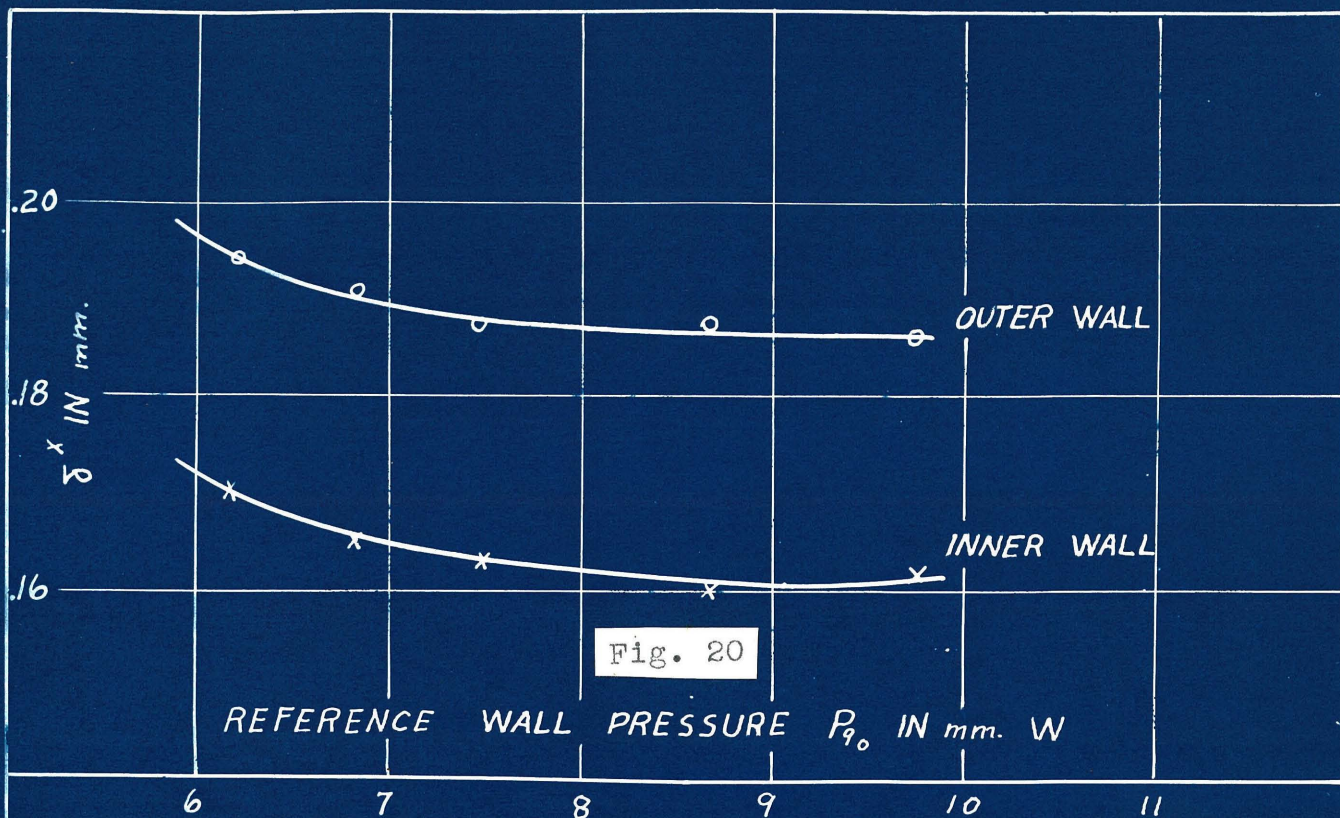
MEASUREMENTS WITH STANTON TUBE

Fig. 21
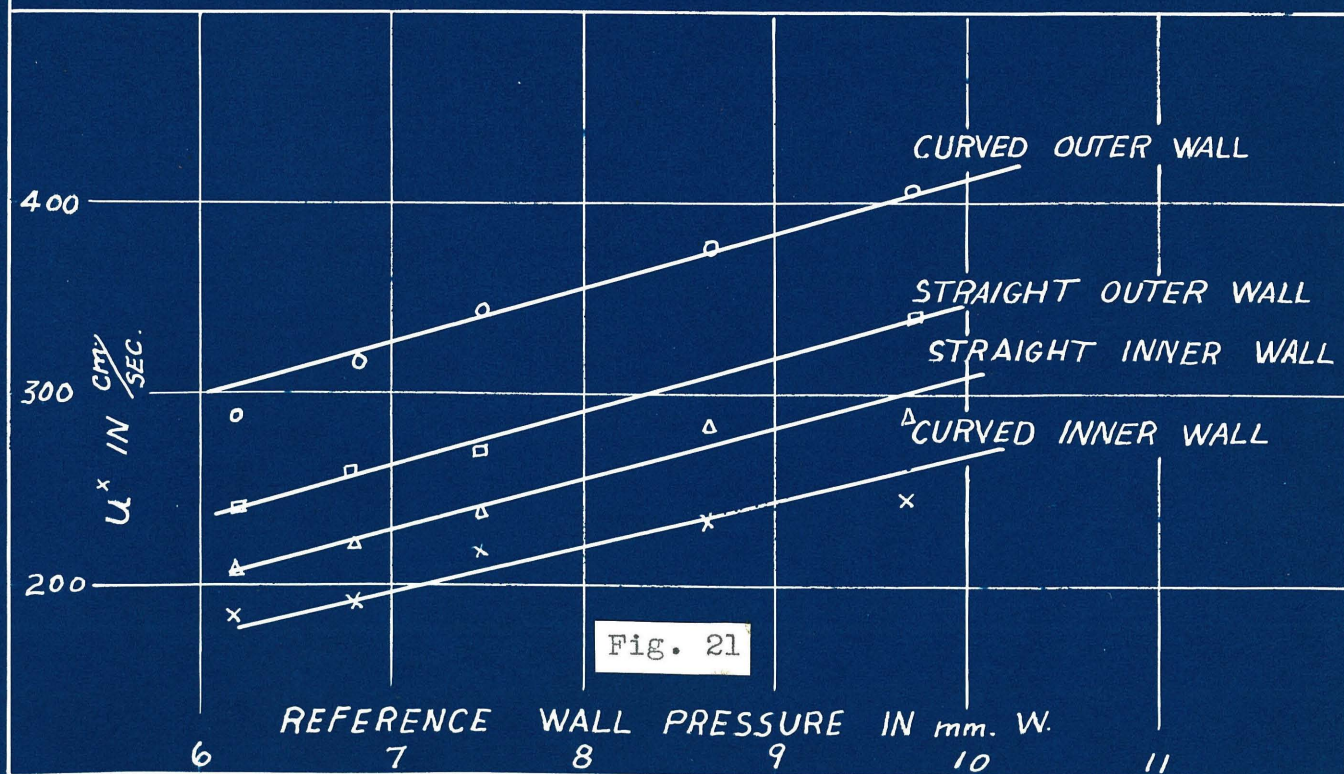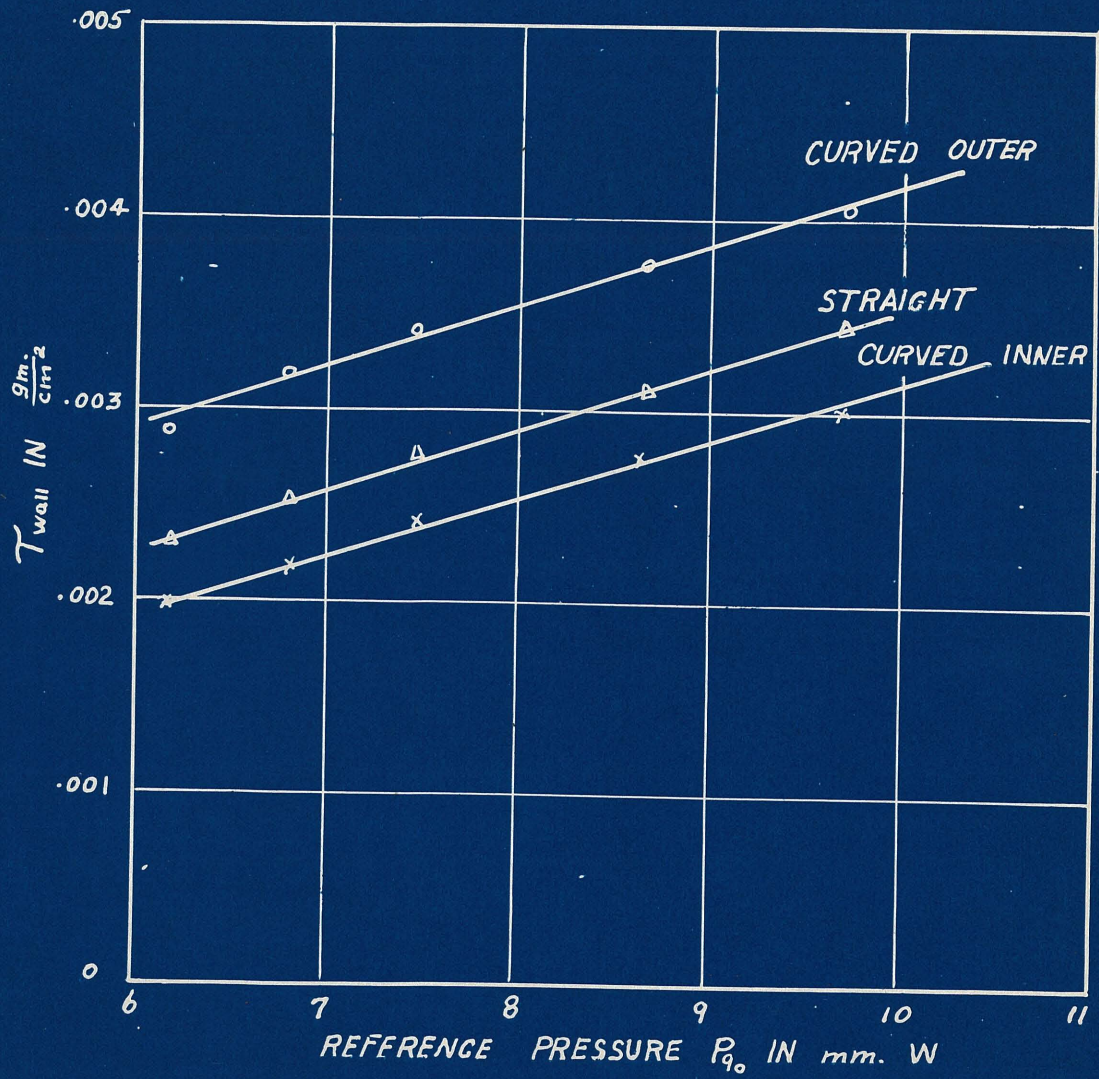
STANTON TUBE MEASUREMENTS FOR τ

Fig. 22
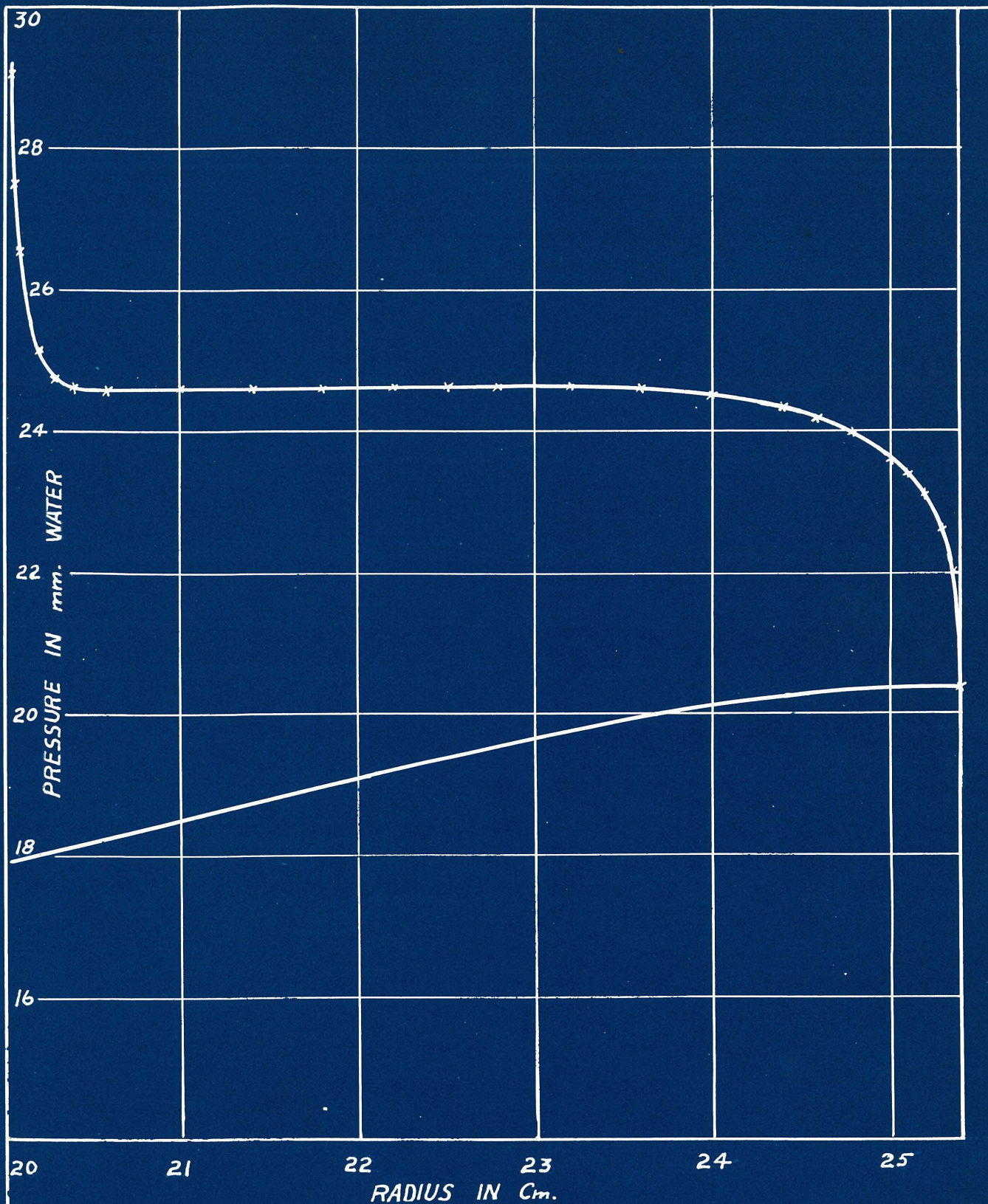
TOTAL HEAD AND STATIC PRESSURE CURVES
FOR CONCENTRIC CYLINDERS

Fig. 23

VELOCITY DISTRIBUTION BETWEEN CONCENTRIC CYLINDERS
INNER CYLINDER ROTATING   OUTER CYLINDER STATIONARY

—o— U_i = 22.8 m/sec
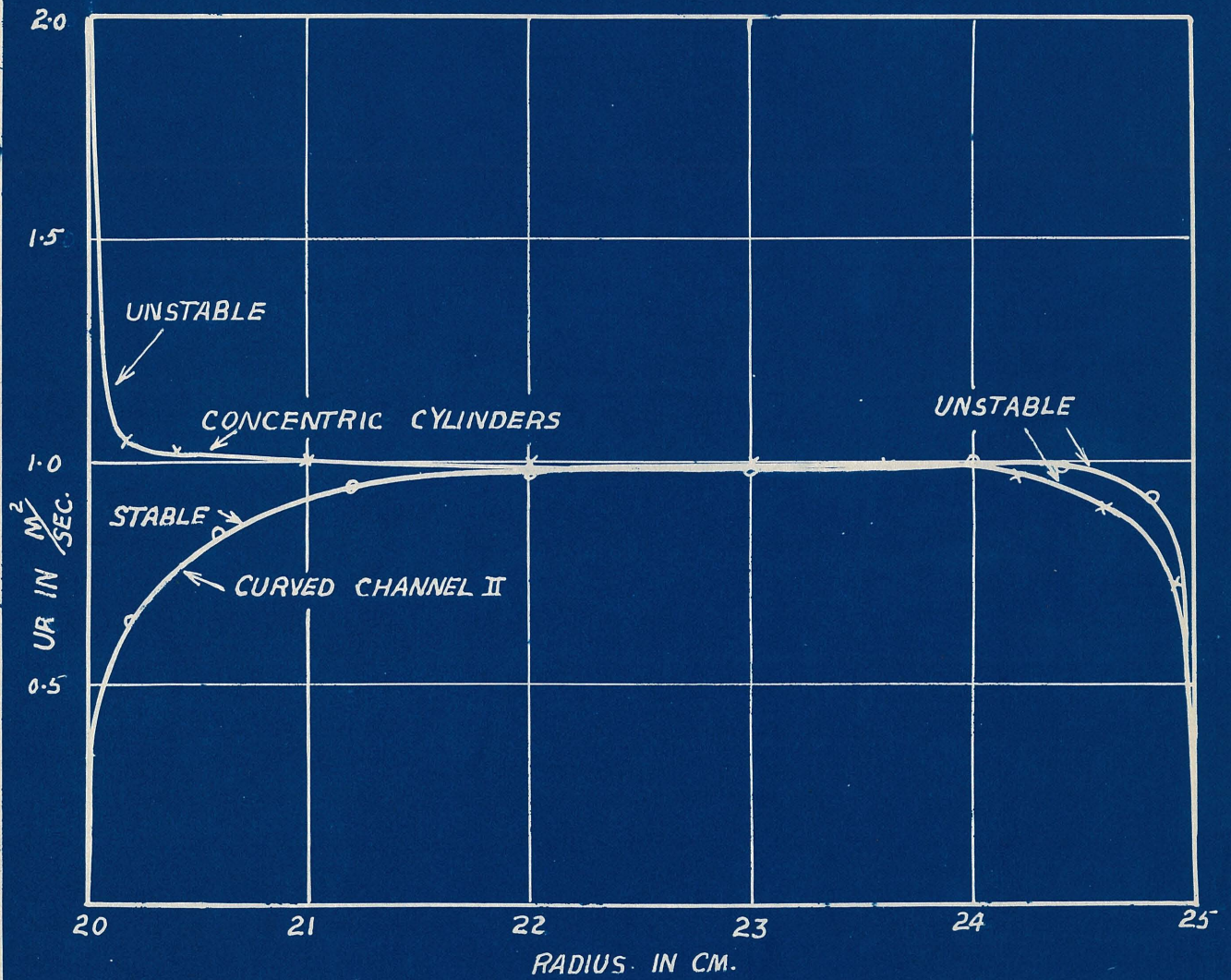—x— U_i = 36.4 m/sec
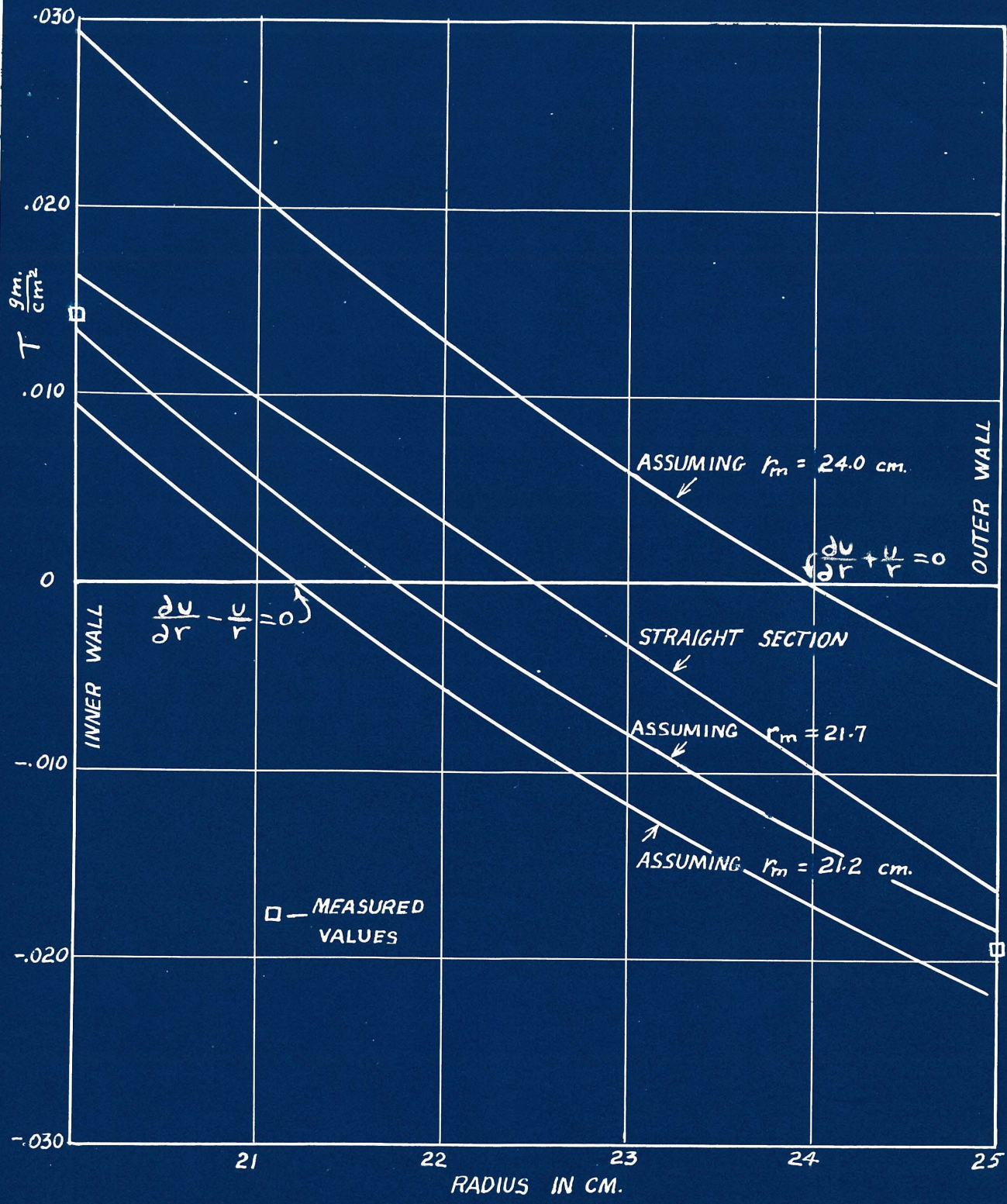U_i = tangential velocity at inner cylinder

Fig. 24

RADIUS IN Cm
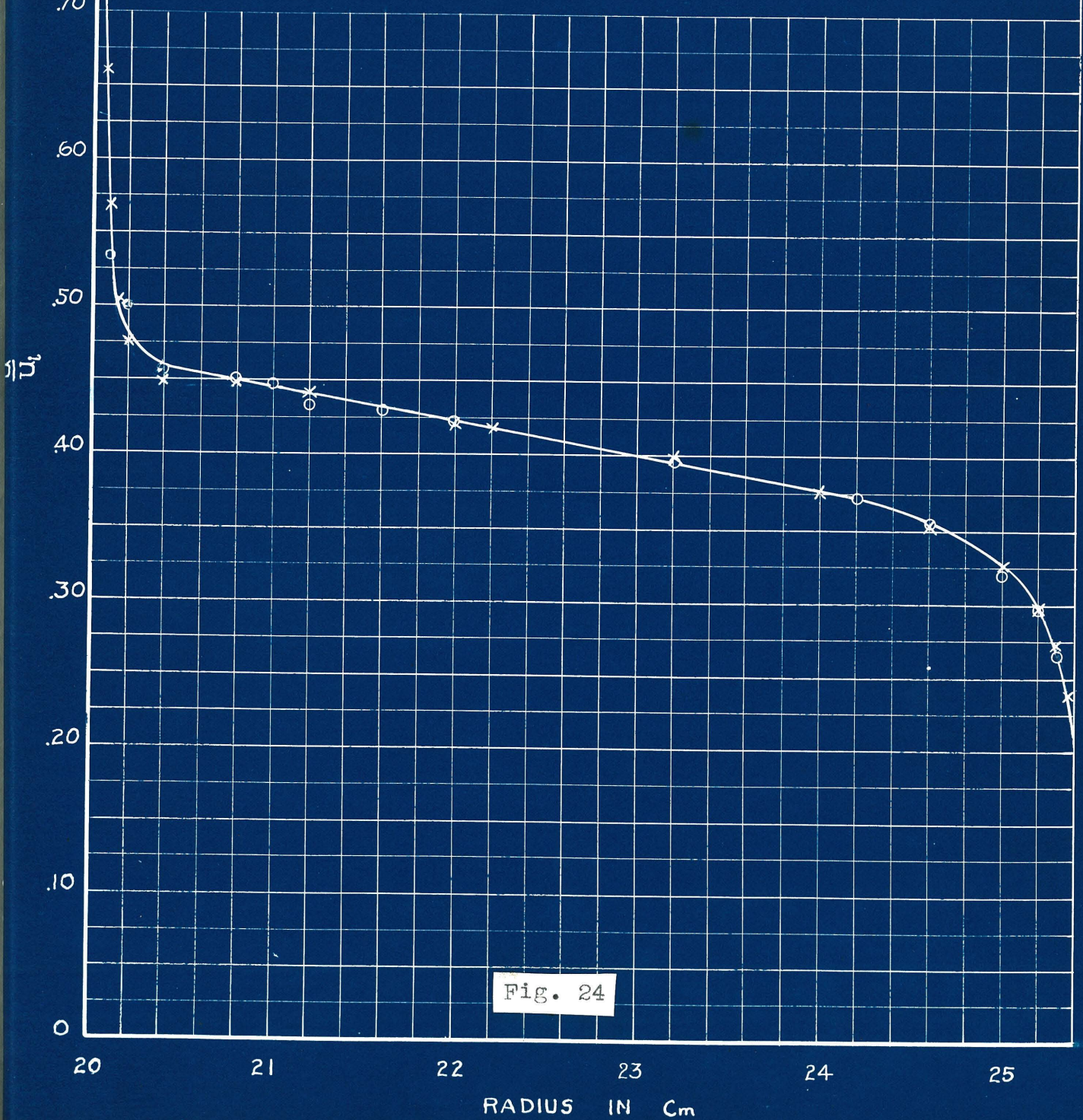
LAMINAR VELOCITY DISTRIBUTION
FOR
CURVED CHANNEL

Case ⓐ $r_i = 20$ $r_o = 25$
Case ⓑ $r_i = 5$ $r_o = 10$
Dotted Line — Straight Flow

$\frac{u}{M} \times \frac{r_o^2 - r_i^2}{\frac{1}{2}r_o^2 r_i^2} \times 10$

30

25

20

15

10

5

0

ⓑ

ⓐ

20   21   22   23   24   25

Radius in Cm.
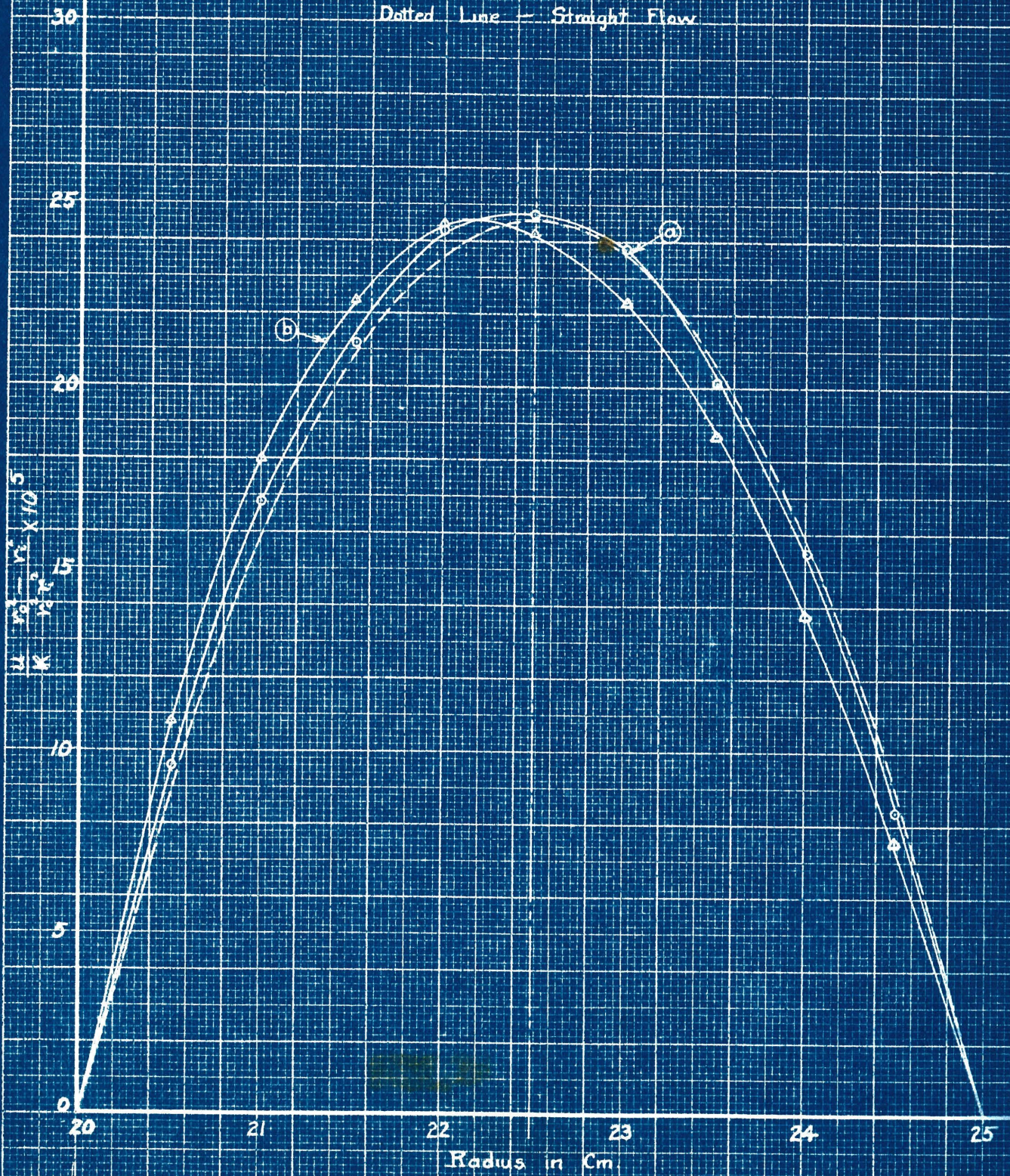
UR CURVES FOR CURVED CHANNEL
AND CONCENTRIC CYLINDERS

Fig. 29

DISTRIBUTION OF Υ FOR CURVED CHANNEL II

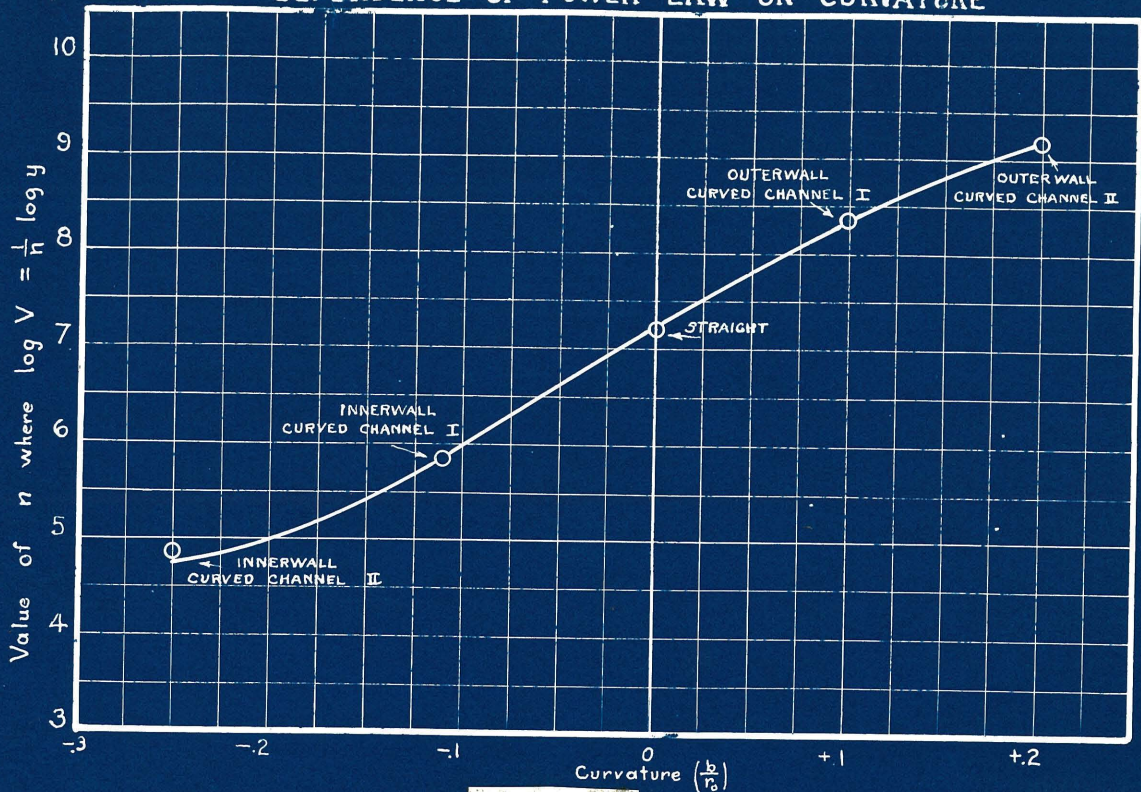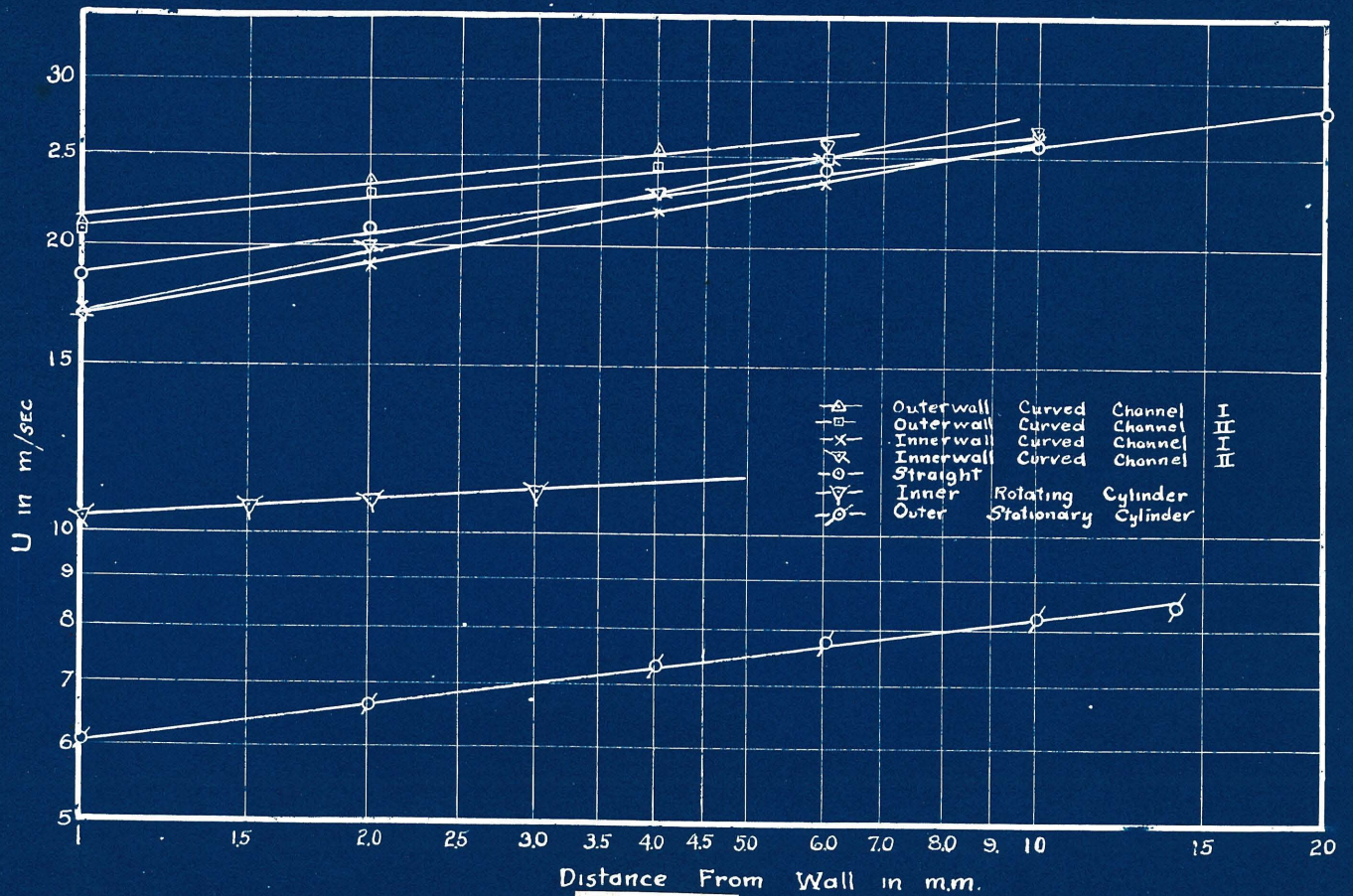Fig. 31

DEPENDENCE OF POWER LAW ON CURVATURE

Fig. 32

Fig. 33

DIMENSIONLESS VELOCITY DISTRIBUTION
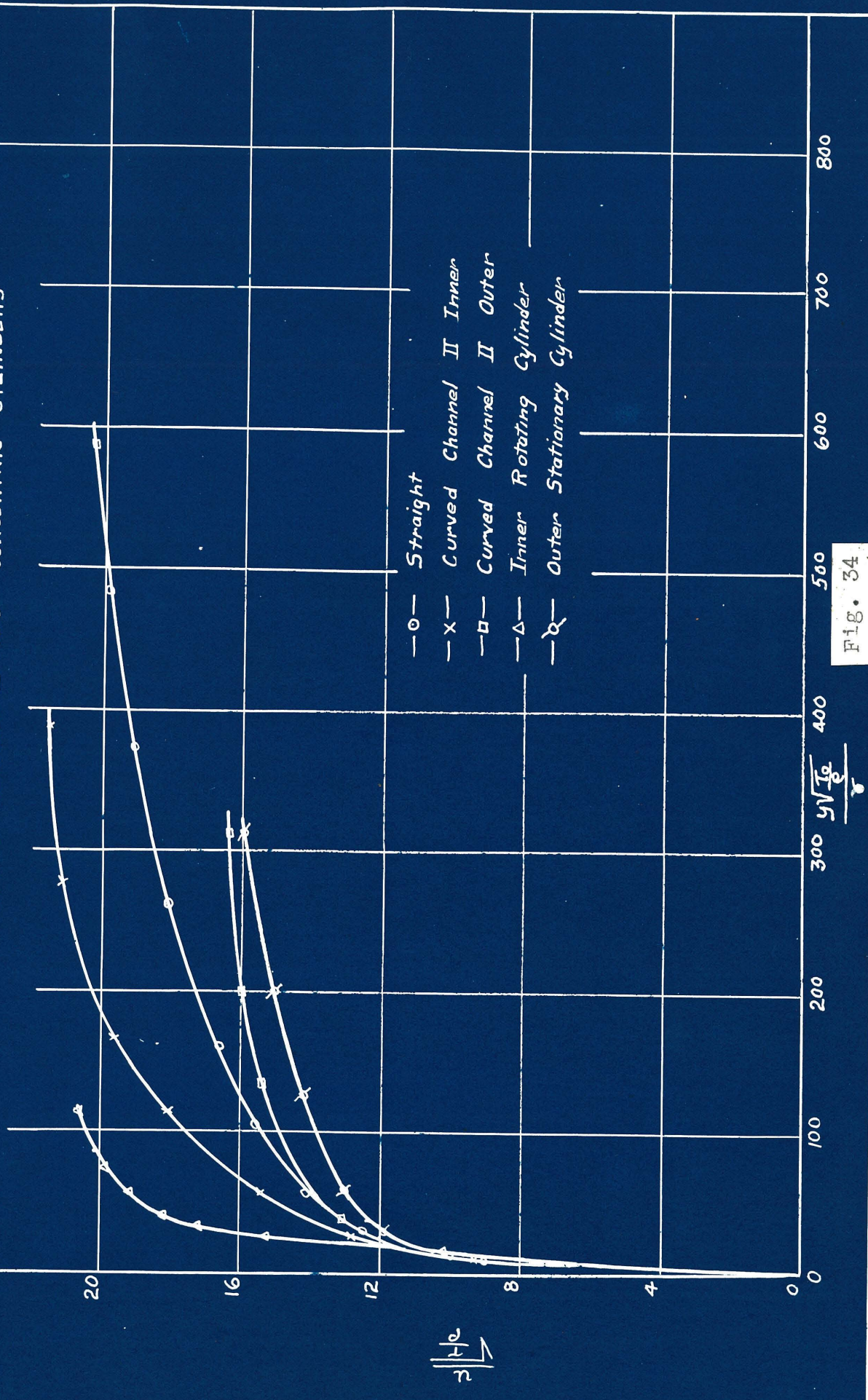NEAR WALL FOR CURVED CHANNEL II AND CONCENTRIC CYLINDERS

—⊙— Straight
—×— Curved Channel II Inner
—□— Curved Channel II Outer
—△— Inner Rotating Cylinder
—○— Outer Stationary Cylinder

Fig. 34
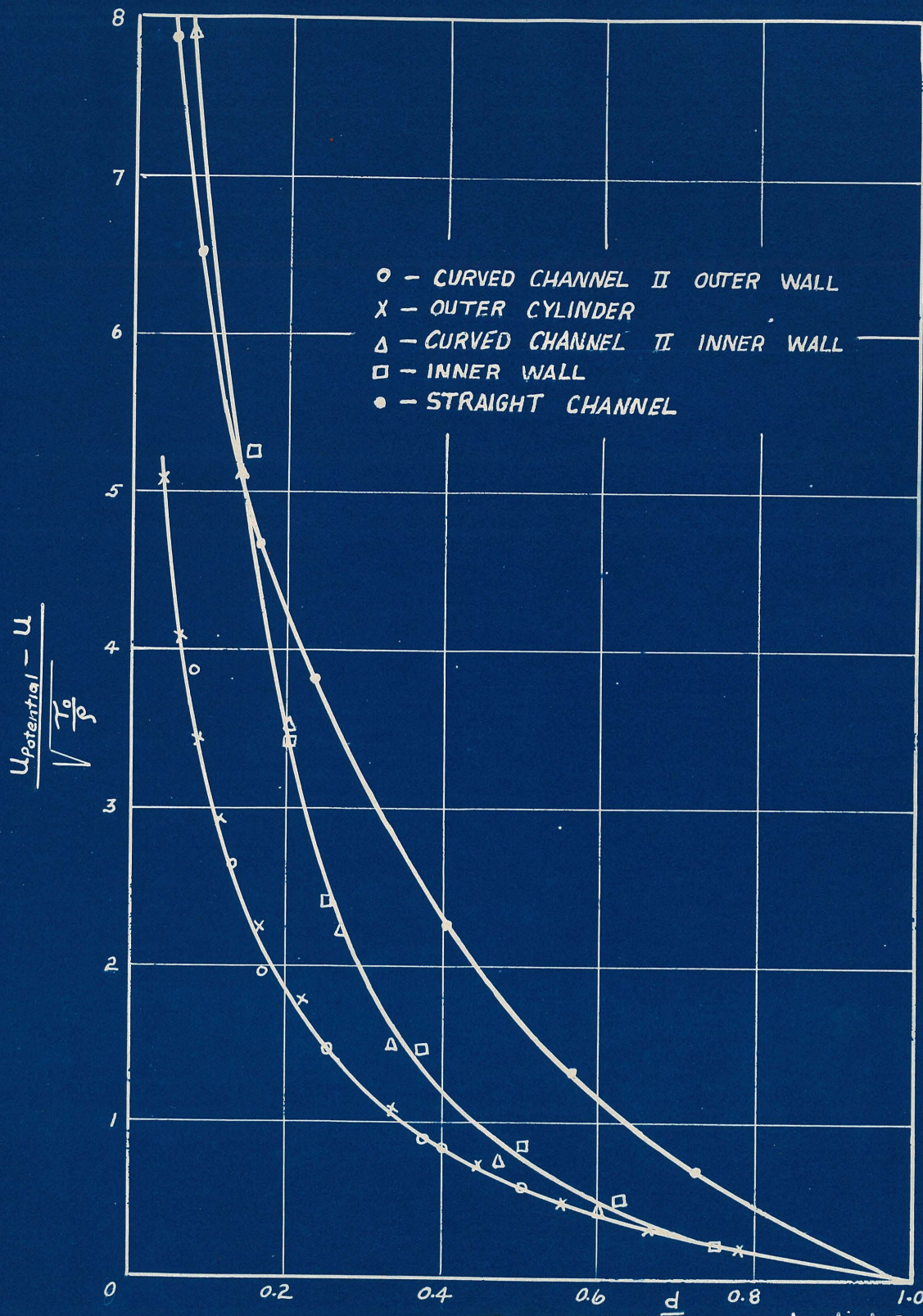
CURVES OF $\dfrac{U_{Potential} - U}{\sqrt{\dfrac{T_o}{\rho}}}$

d = dist. from wall
be = effective breadth

WHERE T_o = MEASURED WALL FRICTION

Legend:
- O – CURVED CHANNEL II OUTER WALL
- X – OUTER CYLINDER
- △ – CURVED CHANNEL II INNER WALL
- □ – INNER WALL
- ● – STRAIGHT CHANNEL